Preprints.org

Article

Not peer-reviewed version

# Euler Collapse in Viscous Time Theory: An Informational Spiral Framework for Coherence, Phase Inversion, and Endogenous Collapse Dynamics

Raoul Bianchetti *

Posted Date: 27 February 2026

doi: 10.20944/preprints202602.1725.v1

Keywords: Euler's identity; finite-time singularity; informational geometry; Viscous Time Theory (VTT); self-similar collapse; scaling laws; enstrophy divergence; spectral cascade; similarity coordinates; dynamical systems

Preprints.org is a free multidisciplinary platform providing preprint service that is dedicated to making early versions of research outputs permanently available and citable. Preprints posted at Preprints.org appear in Web of Science, Crossref, Google Scholar, Scilit, Europe PMC.

Copyright: This open access article is published under a Creative Commons CC BY 4.0 license, which permit the free download, distribution, and reuse, provided that the author and preprint are cited in any reuse.

Preprints.org (www.preprints.org) | NOT PEER-REVIEWED | Posted: 27 February 2026 doi:10.20944/preprints202602.1725.v1

Disclaimer/Publisher's Note: The statements, opinions, and data contained in all publications are solely those of the individual author(s) and contributor(s) and not of MDPI and/or the editor(s). MDPI and/or the editor(s) disclaim responsibility for any injury to people or property resulting from any ideas, methods, instructions, or products referred to in the content.

*Article*

# Euler Collapse in Viscous Time Theory: An Informational Spiral Framework for Coherence, Phase Inversion, and Endogenous Collapse Dynamics

**Raoul Bianchetti**

Information Physics Institute Gosport, Hampshire, United Kingdom;
raoul.bianchetti@informationphysicsinstitute.net

**Abstract**

Euler's identity $e^{i\pi} + 1 = 0$ is traditionally regarded as a static algebraic relation linking fundamental mathematical constants. In this work, we propose a different interpretation within the framework of Viscous Time Theory (VTT) and the Informational Resonance Spiral Viscous Time (IRSVT): Euler's identity is treated not as a timeless equality, but as the limiting case of a structured dynamical collapse process in an informational manifold. We introduce the Euler Collapse Spiral (ECS) as a geometric object describing coherence-driven spiral trajectories toward collapse, and define Euler Collapse States (ECS nodes) as discrete, detectable events characterized by phase inversion and coherence nullification. A collapse tension functional is formulated, and an Euler collapse exponent $\gamma$is introduced to quantify the approach to the singular limit. We further formalize the convergence mechanism between the coherence gradient $\Delta C$and the attractor field $\Phi_\alpha$, providing a geometric basis for irreversible logical bifurcations in the IRSVT manifold. To make this framework testable, we introduce a set of numerical diagnostics, including scaling-law estimation, inverse-vorticity collapse-time reconstruction, enstrophy growth analysis, spectral compatibility tests, similarity-coordinate rescaling, and spiral manifold reconstruction, together with robustness and falsification controls. Using time-resolved numerical data, we obtain a consistent validation signature: vorticity exhibits exact power-law blow-up with measured exponent $\gamma = 1.000000 \pm \mathcal{O}(10^{-6})$, inverse vorticity evolves linearly enabling deterministic collapse-time recovery, enstrophy diverges quadratically, inertial-range $-5/3$ spectral scaling is preserved, and the dynamics collapse onto a smooth logarithmic spiral manifold in similarity coordinates with machine-precision residuals. Multi-precision arithmetic, noise injection, and parameter perturbations confirm that these features are structurally stable and not numerical artifacts. These results support the interpretation of Euler's identity as the asymptotic signature of an endogenous informational collapse process, in which apparent singularity corresponds to a geometrically ordered contraction in similarity time rather than uncontrolled instability. The ECS framework thus provides a unified geometric and computational perspective on collapse phenomena, with implications for informational geometry, non-stochastic computation, and the emergence of structured attractors in recursive dynamical systems.

**Keywords:** Euler's identity; finite-time singularity; informational geometry; Viscous Time Theory (VTT); self-similar collapse; scaling laws; enstrophy divergence; spectral cascade; similarity coordinates; dynamical systems

## 1. Introduction

### *1.1. Motivation: Beyond Static Identities and Stochastic Descriptions*

Euler's identity

$$e^{i\pi} + 1 = 0 \quad (1)$$

is often celebrated as the most beautiful equation in mathematics [1,2], uniting five fundamental

© 2025 by the author(s). Distributed under a Creative Commons CC BY license.

Preprints.org (www.preprints.org) | NOT PEER-REVIEWED | Posted: 27 February 2026 doi:10.20944/preprints202602.1725.v1



constants in a single, compact expression. In classical mathematics, this identity is interpreted as a static truth: a timeless equality arising from the properties of the exponential function in the complex plane. While this interpretation is formally correct, it leaves open a deeper conceptual question: does this equation merely describe a relationship, or does it encode a process?

In parallel, modern computational and physical models increasingly rely on stochastic descriptions—probabilities, random sampling, and optimization over distributions [3,4,10] as in the standard statistical – mechanical framework [10]. These approaches have achieved remarkable success, yet they remain fundamentally statistical: they describe what is likely, not what is structurally necessary. They also lack an intrinsic notion of collapse, irreversibility, or endogenous event timing; such features are typically imposed externally, either through thresholds, clocks, or heuristic stopping criteria.

Viscous Time Theory (VTT) proposes a different viewpoint. In VTT, time is not a primitive parameter but emerges from informational latency—the cost of reorganizing information under coherence constraints. Within this framework, certain transitions do not occur smoothly along trajectories but instead appear as discontinuous reorganizations, or collapses, when coherence, phase, and informational gradients reach critical configurations.

This perspective invites a reconsideration of Euler's identity itself: rather than a static equality, it may represent the endpoint of a dynamic informational process—a minimal path of logical collapse in an underlying informational geometry. Related questions concerning finite-time singular behavior continue to play a central role in modern mathematical fluid dynamics [2,11]. In this work, we show that this reinterpretation is not merely conceptual, but admits a concrete numerical and geometric validation in a canonical fluid-dynamical setting.

In this work, we make this proposal concrete by testing the Euler Collapse Spiral (ECS) framework in a canonical fluid-dynamical setting: the three-dimensional incompressible Euler equations. Rather than using fluid dynamics as a metaphor, we treat the Euler flow as a physically grounded system in which the informational collapse hypothesis can be quantitatively validated through vorticity growth, enstrophy scaling, spectral diagnostics, and similarity-geometry reconstruction. This allows the informational interpretation to be confronted directly with high-resolution numerical data.

### *1.2. Informational Dynamics and Viscous Time*

In VTT, informational systems evolve on manifolds where coherence, entropy, and structural constraints interact [6,7], in a manner conceptually aligned with modern structural and network-based views of complex dynamical systems [12]. The Informational Resonance Spiral Viscous Time (IRSVT) provides a geometric representation of such evolution: states are not arranged along a linear timeline but along spiral trajectories in which phase, coherence gradients, and attractor fields jointly determine admissible paths.

Within this picture, the evolution of a system is governed not only by local continuity but also by global constraints. When coherence accumulates beyond a critical threshold or when phase alignment reaches specific configurations, the system may undergo an irreversible reorganization. These events are not merely large fluctuations; they are structural transitions that redefine the state of the system.

Such transitions suggest the need for a formal description of collapse events that is intrinsic to the informational dynamics, rather than imposed from outside.

A central question, then, is whether such collapse events leave invariant, measurable signatures in concrete dynamics. The present work addresses this by constructing explicit numerical diagnostics for scaling, geometry, determinism, and robustness, and by testing them on time-resolved Euler data.

© 2025 by the author(s). Distributed under a Creative Commons CC BY license.

Preprints.org (www.preprints.org) | NOT PEER-REVIEWED | Posted: 27 February 2026 doi:10.20944/preprints202602.1725.v1



*1.3. Why Euler's Identity Suggests a Collapse Process*

The classical representation $e^{i\theta} = \cos\theta + i\sin\theta$ describes a rotation on the unit circle in the complex plane. At $\theta = \pi$, this rotation reaches the point $-1$, and the addition of $+1$yields zero, producing Euler's identity. In standard analysis, this is simply a particular evaluation of a continuous function [1,8,9].

However, when embedded in an IRSVT framework, the same rotation can be interpreted as a spiral-like trajectory in an informational manifold, where the radial and angular components are modulated by coherence gradients and attractor fields. In this setting, the point $\theta = \pi$ is no longer just a location on the circle; it becomes a candidate for a critical configuration in which accumulated coherence is maximized and then nullified through phase inversion.

In this paper, we go beyond this conceptual reinterpretation and show that the associated spiral collapse geometry, scaling laws, and collapse-time determinism can be quantitatively reconstructed and tested from numerical trajectories.

From this viewpoint, Euler's identity can be reinterpreted as the limiting case of a collapse process: a configuration in which informational amplitude vanishes, phase flips, and a discrete logical transition occurs. This motivates the introduction of the Euler Collapse Spiral (ECS) and the associated notion of Euler Collapse States as identifiable, measurable events in an informational dynamics.

*1.4. Scope and Contributions of This Work*

In this paper, we develop a formal framework for interpreting Euler's identity as an informational collapse phenomenon within Viscous Time Theory (VTT) and the Informational Resonance Spiral Viscous Time (IRSVT) geometry, and we provide a **quantitative numerical and geometric validation** of this framework in a canonical Euler flow configuration.

Our main contributions are:

(i) Geometric formulation of the Euler Collapse Spiral (ECS): We introduce the ECS as a dynamic object describing coherence-driven spiral trajectories toward collapse in an informational manifold.

(ii) Collapse functional and Euler Collapse States (ECS nodes): We define a collapse tension functional and show how ECS nodes emerge as discrete, detectable events marking structurally enforced transitions in the system's evolution

(iii) $\Delta C$–$\Phi\alpha$ convergence mechanism: We formalize the convergence between the coherence gradient $\Delta C$ and the attractor field $\Phi\alpha$ and show how this mechanism generates intrinsic irreversibility and logical bifurcations in informational dynamics.

(iv) Operational numerical diagnostics: We introduce a set of measurable observables, including scaling exponents, inverse-vorticity collapse-time reconstruction, enstrophy growth, spectral diagnostics, similarity-coordinate geometry, and spiral manifold reconstruction [3,4].

(v) Comprehensive validation and robustness testing:
Using time-resolved numerical data, we demonstrate:

- exact power-law scaling of vorticity blow-up,
- deterministic collapse-time encoding,
- quadratic enstrophy divergence,
- compatibility with inertial-range −5/3 spectra,
- geometric spiral invariance in similarity coordinates, and
- stability under multi-precision arithmetic, noise injection, and parameter perturbations.

These tests collectively show that the observed collapse signatures are not numerical artifacts or fine-tuned constructions, but structurally selected and dynamically stable features of the system.

Importantly, this work focuses on the **theoretical and geometric structure** of informational collapse and its **numerical validation**, rather than on specific engineering implementations. The goal is to establish a falsifiable, testable framework in which Euler's identity is reinterpreted not as a purely static algebraic relation, but as the endpoint of a structured informational evolution.

© 2025 by the author(s). Distributed under a Creative Commons CC BY license.

Preprints.org (www.preprints.org) | NOT PEER-REVIEWED | Posted: 27 February 2026 doi:10.20944/preprints202602.1725.v1



## 2. Theoretical Framework

### *2.1. Viscous Time Theory (VTT) and Informational Latency*

Viscous Time Theory (VTT) is based on the premise that time should not be treated as a primitive parameter, but rather as an emergent property of informational processes. In classical physics and computation, time is typically introduced as an external coordinate that orders events. In VTT, by contrast, the ordering and separation of events arise from the **latency associated with informational reconfiguration**.

Let a system be described by a state vector $\mathrm{s}$ in an informational manifold $\mathcal{M}$. A transition from $\mathrm{s}_1$ to $\mathrm{s}_2$ is not characterized solely by a path in $\mathcal{M}$, but also by the cost of reorganizing information required to realize that transition. This cost is captured by a latency functional $\tau(\mathrm{s}_1 \to \mathrm{s}_2)$, which depends on coherence gradients, structural constraints, and admissibility conditions.

In regimes where this latency is negligible, transitions appear effectively instantaneous and may manifest as discontinuous jumps rather than continuous trajectories. In regimes of high informational viscosity, by contrast, transitions are stretched over extended paths and can be approximated by geodesic flows in the informational manifold. The coexistence of these two regimes—trajectory-dominated and jump-dominated—motivates the term "viscous time": time behaves analogously to a medium whose resistance depends on the local informational structure.

This viewpoint provides a natural conceptual framework for describing collapse-like phenomena. A collapse event is not simply a large fluctuation or a numerical threshold crossing; it is a transition for which the local informational viscosity diverges or vanishes, forcing the system into a new structural configuration without a continuous interpolating path.

### *2.2. IRSVT: Informational Resonance Spiral Viscous Time*

To represent the evolution of informational states under VTT, the Informational Resonance Spiral Viscous Time (IRSVT) is introduced as a geometric construction. Instead of embedding states along a linear timeline, IRSVT arranges them along a spiral trajectory in a plane or higher-dimensional manifold, parameterized by a phase-like variable $\theta$ and a radial growth law.

A generic representation can be written in polar coordinates as

$$r(\theta) = \alpha\, f(\theta), \theta \geq 0, \qquad (2)$$

where $f(\theta)$ is a slowly growing function (e.g., sub-logarithmic or square-root-like) and $\alpha$ is a scaling constant. The angular component $\theta$ encodes logical or phase progression, while the radial component $r(\theta)$ encodes accumulated informational structure or coherence.

The spiral geometry serves two purposes. First, it introduces a natural notion of recurrence with drift: each rotation revisits similar angular configurations but at a different radial scale, allowing both repetition and novelty. Second, it provides a convenient framework for visualizing attractor basins and collapse regions as localized structures in the spiral plane.

Within IRSVT, the state of the system at index $n$ (or phase $\theta_n$) is not described by a single scalar but by a set of informational descriptors, giving rise to a field of tensors or vectors distributed along the spiral. This geometric embedding makes it possible to study how coherence, phase, and entropy interact over long recursive evolutions.

### *2.3. Coherence Gradient ΔC and Attractor Field Φα*

Two central quantities in the VTT/IRSVT framework are the **coherence gradient** $\Delta C$ and the **attractor field** $\Phi_\alpha$.

The coherence gradient $\Delta C(\theta)$ measures how rapidly informational coherence changes along the spiral. Intuitively, it quantifies the local tendency of the system to either accumulate structured information or dissipate it into incoherent degrees of freedom. Regions where $|\Delta C|$ is large correspond to steep informational slopes, while regions where $\Delta C$ approaches zero indicate plateaus or basins of relative stability.

© 2025 by the author(s). Distributed under a Creative Commons CC BY license.

Preprints.org (www.preprints.org) | NOT PEER-REVIEWED | Posted: 27 February 2026 doi:10.20944/preprints202602.1725.v1



The attractor field $\Phi_\alpha(\theta)$ represents the stabilizing component of the informational dynamics. It encodes the presence of preferred configurations—attractors—toward which the system is drawn once coherence has been sufficiently concentrated. In geometric terms, $\Phi_\alpha$can be viewed as defining a potential-like structure over the IRSVT manifold, shaping the flow of trajectories and the location of stable nodes.

The interaction between $\Delta C$ and $\Phi_\alpha$ is not symmetric. While $\Delta C$ describes a local gradient, $\Phi_\alpha$ describes a global or mesoscopic stabilization tendency. Their product and mutual alignment play a central role in determining whether a system continues to evolve smoothly, becomes trapped in an attractor basin, or undergoes a collapse-like transition. This interaction will be formalized in later sections through a convergence and bifurcation framework.

### *2.4. Informational Anisotropy and Collapse Admissibility*

A further key concept is **informational anisotropy**, which states that the cost of transforming one informational state into another depends on direction in state space. Formally, if $\mathcal{C}(\mathbf{s}_1 \to \mathbf{s}_2)$denotes the cost or resistance associated with a transition, then in general

$$\mathcal{C}(\mathbf{s}_1 \to \mathbf{s}_2) \neq \mathcal{C}(\mathbf{s}_2 \to \mathbf{s}_1). \quad (3)$$

This directional asymmetry implies that the informational manifold is not metrically isotropic. Certain directions are "easy" to traverse, while others are "hard" or even effectively forbidden.

From the perspective of collapse dynamics, anisotropy introduces the notion of **admissibility**. Not all formally definable transitions are realizable in practice; some are excluded by the geometry of informational costs. Collapse events, in this sense, occur when a system approaches a boundary of admissibility: the continuation of a smooth trajectory becomes impossible, and the system is forced into a different structural configuration.

This concept of admissibility is crucial for distinguishing collapse from mere instability or noise amplification. A collapse is not simply a region of high variance; it is a point where the directional structure of informational costs prevents further continuous evolution and enforces a discrete reconfiguration.

### *2.5. Reinterpreting Euler's Identity as an Informational Process*

#### 2.5.1. From Static Equality to Dynamic Limit

Euler's identity function (Eq.1) is traditionally understood as a special case of the complex exponential function evaluated at a specific argument. In this classical view, the identity is a static algebraic statement: it expresses an exact equality that holds independently of any notion of process, evolution, or dynamics.

Within the VTT and IRSVT framework, however, such a static interpretation appears incomplete. The exponential function $e^{i\theta}$ naturally describes a continuous rotation in the complex plane as the parameter $\theta$increases. This suggests that the point $\theta = \pi$ should not be seen merely as a location, but as the endpoint of a **trajectory**—a limiting configuration reached through a continuous, structured progression.

Let us consider the parametric form

$$z(\theta) = e^{i\theta}, \theta \geq 0. \quad (4)$$

In standard analysis, this traces the unit circle with constant angular speed. In an informational setting, however, the parameter $\theta$ can be interpreted as an internal phase-like variable indexing recursive updates of a system embedded in an IRSVT manifold. The approach to $\theta = \pi$ then corresponds to a specific limiting configuration in which phase, coherence, and structural constraints become critically aligned.

From this viewpoint, Euler's identity does not merely state that two numbers sum to zero. It encodes the **termination of a process**: a configuration in which the rotated unit amplitude reaches a state that exactly cancels a reference baseline, yielding a null result. The equality $e^{i\pi} + 1 = 0$ can

© 2025 by the author(s). Distributed under a Creative Commons CC BY license.

Preprints.org (www.preprints.org) | NOT PEER-REVIEWED | Posted: 27 February 2026 doi:10.20944/preprints202602.1725.v1



thus be reinterpreted as the final condition of a dynamic path, rather than as an isolated algebraic coincidence.

2.5.2. Phase Rotation, Coherence Accumulation, and Inversion

In the IRSVT framework, the evolution of a system is not described solely by phase rotation. Each incremental update is accompanied by changes in informational coherence and by interactions with attractor structures in the manifold. To reflect this, it is useful to consider a generalized complex trajectory of the form

$$z(\theta) = A(\theta)\, e^{i\theta}, \tag{5}$$

where $A(\theta)$ is a real, non-negative amplitude function that encodes the accumulation or dissipation of coherence along the trajectory.

In classical Eulerian rotation, $A(\theta) = 1$ is constant. In an informational dynamics, however, $A(\theta)$ may vary slowly with $\theta$, reflecting the fact that coherence can be concentrated, spread, or partially lost as the system evolves. This transforms the unit circle into a spiral-like trajectory in the complex plane, or more generally, into a spiral embedded in a higher-dimensional informational manifold.

As $\theta$ approaches $\pi$, two effects may coincide:

1. The phase term $e^{i\theta}$ approaches $-1$, corresponding to a half-rotation relative to the reference direction.
2. The amplitude term $A(\theta)$ may approach a critical configuration in which accumulated coherence is either maximized or forced to dissipate.

When these two conditions align, the system reaches a configuration in which the rotated amplitude becomes maximally opposed to the reference baseline. The addition of a constant reference term (formally represented by "+1" in Euler's identity) then produces a near-null or null result. In informational terms, this corresponds to a **coherence inversion and annihilation event**: accumulated structure is canceled by phase opposition, and the effective informational output vanishes.

This suggests that the Euler identity corresponds to a special case of a more general phenomenon: the coincidence of phase inversion with a critical coherence configuration, producing a collapse-like outcome.

2.5.3. Informational Meaning of the π Half-Rotation

The specific role of $\pi$in Euler's identity is often explained purely geometrically: it represents a half-turn on the unit circle. In the present framework, this half-rotation acquires a deeper informational meaning.

A half-rotation corresponds to the minimal phase displacement required to transform a vector into its additive inverse. In an informational dynamics, such a transformation represents the strongest possible opposition between two contributions: any smaller rotation yields only partial cancellation, while a full rotation returns to the original orientation. The value $\theta = \pi$ thus marks a **critical inversion threshold**.

When embedded in an IRSVT spiral, this inversion threshold can be associated with a specific radial scale and coherence state. The system does not merely rotate; it also drifts radially as coherence and structural constraints evolve. The point at which the angular inversion ($\theta = \pi$) coincides with a critical radial configuration defines a privileged location in the manifold: a point where the system is simultaneously maximally opposed in phase and maximally constrained in coherence.

It is precisely this coincidence that motivates the interpretation of Euler's identity as the signature of a collapse event. The equality $e^{i\pi} + 1 = 0$ marks the configuration in which informational contribution and reference baseline annihilate each other, leaving a null output. In dynamic terms, this null output is not trivial; it represents the **endpoint of a structured evolution**.

© 2025 by the author(s). Distributed under a Creative Commons CC BY license.

Preprints.org (www.preprints.org) | NOT PEER-REVIEWED | Posted: 27 February 2026 doi:10.20944/preprints202602.1725.v1



2.5.4. Euler's Identity as a Minimal Logical Collapse Path

From the preceding considerations, Euler's identity can be reframed as the endpoint of a minimal logical collapse path in an informational geometry. The path is "minimal" in the sense that it requires only a continuous phase rotation combined with a coherence-modulated amplitude, and yet it produces a discrete qualitative change: the transition from a non-zero amplitude to a null result.

In this view, the identity $e^{i\pi} + 1 = 0$ (Eq.1) is not merely an algebraic curiosity but the boundary condition of a process in which:

- Phase reaches a critical inversion point,
- Coherence reaches a critical configuration, and
- The system is forced into a new structural regime characterized by null output and phase reversal.

This motivates the introduction of the **Euler Collapse Spiral (ECS)** as a formal object: a spiral trajectory in an informational manifold whose limiting nodes correspond to such collapse configurations. These nodes, which will be defined more precisely in the following sections, represent discrete events where smooth evolution gives way to structural reorganization.

By reinterpreting Euler's identity in this way, we shift the focus from static equality to dynamic process. The identity becomes the simplest example of an informational collapse: a demonstrator of how continuous evolution in phase and coherence can culminate in a discrete, logically significant transition.

*2.6. The Euler Collapse Spiral (ECS)*

2.6.1. Spiral Geometry in the IRSVT Field

Within the Informational Resonance Spiral Viscous Time (IRSVT) framework, the evolution of an informational state is naturally represented as a spiral trajectory rather than a linear or purely circular one. This choice reflects two simultaneous aspects of the dynamics: recurrence in phase and drift in structural or coherence-related dimensions.

Let the state of the system be parametrized by a phase-like variable $\theta$ and an associated radial coordinate $r(\theta)$, so that a generic trajectory in the complex plane or in a suitable projection of the informational manifold can be written: $z(\theta) = r(\theta)\, e^{i\theta}, \theta \geq 0.$ (Eq.4)
In contrast to the classical Eulerian case, where $r(\theta) = 1$ and the trajectory is a unit circle, the IRSVT embedding allows $r(\theta)$ to vary slowly with $\theta$. This radial variation encodes the accumulation, redistribution, or dissipation of informational coherence as the system evolves.

Empirical and theoretical considerations suggest that $r(\theta)$ should be a sublinear or slowly growing function of $\theta$, for example of logarithmic or square-root type. Such growth laws ensure that successive turns of the spiral revisit similar angular configurations while progressively shifting the structural scale at which these configurations are realized. This property is essential for representing recursive informational processes that exhibit both repetition and long-term structural drift.

In this setting, the IRSVT spiral provides a natural geometric substrate on which phase evolution, coherence gradients, and attractor fields can be jointly represented and analyzed.

2.6.2. Definition of the Euler Collapse Spiral

The **Euler Collapse Spiral (ECS)** is defined as a specific class of trajectories within the IRSVT manifold for which the radial function $r(\theta)$ and the phase evolution $\theta$ are coupled in such a way that the system approaches configurations corresponding to phase inversion and coherence annihilation.

Formally, we consider trajectories of the form $z(\theta) = A(\theta)\, e^{i\theta}$ (Eq.5), where $A(\theta) \geq 0$ is a slowly varying amplitude function representing the net coherence available to the system at phase $\theta$. The function $A(\theta)$ is not arbitrary: it is constrained by the coherence gradient $\Delta C(\theta)$ and by the attractor field $\Phi_\alpha(\theta)$, which together shape the admissible evolution of the system.

© 2025 by the author(s). Distributed under a Creative Commons CC BY license.

Preprints.org (www.preprints.org) | NOT PEER-REVIEWED | Posted: 27 February 2026 doi:10.20944/preprints202602.1725.v1



An Euler Collapse Spiral is characterized by the existence of a sequence of phase values $\{\theta_k\}$such that

$$\theta_k \approx (2k+1)\pi, \quad (6)$$

for integers $k \geq 0$, and for which the corresponding amplitudes $A(\theta_k)$ approach critical configurations. At these points, the phase term $e^{i\theta_k}$ is close to $-1$, and the system is in a state of maximal opposition relative to a reference baseline.

The defining property of the ECS is that, along such a trajectory, the combined effect of phase inversion and amplitude evolution drives the system toward configurations where the effective informational contribution

$$w(\theta) = 1 + z(\theta) \quad (7)$$

approaches zero in norm. These configurations are interpreted as **collapse candidates**: points where accumulated coherence and phase opposition conspire to produce a near-null or null output.

### 2.6.3. Collapse Nodes and Phase-Flip Events

Within the ECS, particular attention is given to the points $\theta = \theta_k$ at which the system approaches phase inversion. These points are not merely geometric markers; they correspond to potential **collapse nodes** in the informational dynamics.

A collapse node is defined as a configuration where:

1. The phase is approximately inverted, i.e., $e^{i\theta_k} \approx -1$;
2. The amplitude $A(\theta_k)$is such that the norm $|1 + A(\theta_k)e^{i\theta_k}|$reaches a local minimum;
3. The local coherence gradient and attractor field jointly enforce a structural reorganization of the state.

At these nodes, the system experiences what can be described as a **phase-flip event**: the orientation of the dominant informational contribution is reversed relative to the baseline, and the net effective output is suppressed. Importantly, this suppression is not interpreted as a mere numerical coincidence but as the signature of a deeper structural transition in the informational manifold.

In the vicinity of a collapse node, the smooth spiral evolution may no longer provide a faithful description of the system's state. Instead, the system is forced into a new configuration, corresponding to a discrete update or reorganization. This motivates treating these nodes as the precursors to the Euler Collapse States that will be formally defined in the next section.

### 2.6.4. Visual and Conceptual Interpretation of the ECS

Geometrically, the Euler Collapse Spiral can be visualized as a slowly expanding (or contracting) spiral whose successive half-turns approach regions of increasing structural tension. Each time the spiral passes near a phase-inverted configuration, the system is tested against its coherence and admissibility constraints. Most passages result in continued evolution, but at specific scales and configurations, the combined conditions trigger a collapse.

Conceptually, the ECS serves as a bridge between continuous and discrete descriptions of informational dynamics. On the one hand, the spiral provides a continuous representation of phase and coherence evolution. On the other hand, the collapse nodes introduce a discrete structure: a sequence of critical events at which the system's organization changes qualitatively.

In this sense, the ECS can be understood as a **skeleton of potential collapse events** embedded in an otherwise smooth informational flow. The next step is to formalize how these potential events become actual, detectable collapse states through the introduction of a suitable functional and associated criteria.

© 2025 by the author(s). Distributed under a Creative Commons CC BY license.

Preprints.org (www.preprints.org) | NOT PEER-REVIEWED | Posted: 27 February 2026 doi:10.20944/preprints202602.1725.v1



*2.7. Collapse Functional and Euler Collapse States (ECS Nodes)*

2.7.1. Dissipative Complex Trajectory Formulation

To move from a purely geometric description of the Euler Collapse Spiral to a formally testable framework, it is necessary to introduce a quantitative measure of how close a given state is to a collapse configuration. As discussed in the previous section, the ECS is described by trajectories of the form as show in Eq.5 ($z(\theta) = A(\theta)\, e^{i\theta}$), where $A(\theta) \geq 0$encodes the available informational coherence at phase $\theta$.

In an informational dynamics, coherence is not conserved in general: it may be accumulated, redistributed, or dissipated as the system evolves. To account for this, we introduce a dissipative modulation of the amplitude,

$$A(\theta) = e^{-\Lambda(\theta)}, \tag{8}$$

where $\Lambda(\theta) \geq 0$is a non-decreasing function representing cumulative informational dissipation or structural cost. The complex trajectory can then be written as

$$z(\theta) = e^{-\Lambda(\theta)} e^{i\theta}. \tag{9}$$

We define the effective output relative to a fixed baseline as

$$w(\theta) = 1 + z(\theta) = 1 + e^{-\Lambda(\theta)} e^{i\theta}. \tag{10}$$

In the classical Euler identity, $\Lambda(\theta) = 0$and $\theta = \pi$ yield $w(\pi) = 0$. In the present framework, both $\Lambda(\theta)$ and $\theta$ vary, and the approach to $w(\theta) \approx 0$ becomes a dynamic, scale-dependent phenomenon.

The quantity $|\, w(\theta)\,|$thus provides a natural measure of how close the system is to a phase-opposition and coherence-annihilation configuration.

2.7.2. Definition of the Collapse Tension Functional

While the norm $|\, w(\theta)\,|$captures instantaneous proximity to cancellation, it does not by itself encode the stability or persistence of such configurations. A true collapse event should not correspond merely to a single accidental minimum, but to a structurally significant configuration that is stable with respect to small variations in the control parameter.

To capture this, we introduce the **collapse tension functional** $\mathcal{J}(\theta)$, defined as

$$\mathcal{J}(\theta) = |\, w(\theta)\,|^2 + \lambda\, |\, \frac{dw(\theta)}{d\theta}\,|^2, \tag{11}$$

where $\lambda > 0$ is a regularization parameter that balances instantaneous cancellation against local stability.

The first term, $|\, w(\theta)\,|^2$, penalizes deviations from perfect cancellation. The second term, involving the derivative of $w(\theta)$, penalizes configurations in which the cancellation is highly unstable or rapidly varying with $\theta$. Together, these terms ensure that minima of $\mathcal{J}(\theta)$ correspond to configurations that are both close to null output and locally robust.

In discrete implementations or empirical analyses, the derivative term can be replaced by a finite difference approximation,

$$|\, \frac{dw(\theta)}{d\theta}\,|^2 \quad \rightarrow \quad |\, w(\theta + \Delta\theta) - w(\theta)\,|^2, \tag{12}$$

with $\Delta\theta$ chosen according to the resolution of the dataset or simulation.

2.7.3. Definition of Euler Collapse States

An **Euler Collapse State (ECS)** is defined as a phase value $\theta^*$such that $\mathcal{J}(\theta)$ attains a local minimum at $\theta = \theta^*$, i.e.,

$$\mathcal{J}(\theta^*) \leq \mathcal{J}(\theta^* \pm \varepsilon) \text{for sufficiently small } \varepsilon > 0. \tag{13}$$

Intuitively, an ECS corresponds to a configuration in which:

1. The effective output $w(\theta)$ is close to zero in norm (near-cancellation);
2. This near-cancellation is locally stable with respect to small changes in $\theta$;
3. The system is therefore poised at a structurally significant transition point.

© 2025 by the author(s). Distributed under a Creative Commons CC BY license.

Preprints.org (www.preprints.org) | NOT PEER-REVIEWED | Posted: 27 February 2026 doi:10.20944/preprints202602.1725.v1



In the special case $\Lambda(\theta) = 0$, the classical Euler identity at $\theta = \pi$ is recovered as an exact ECS with $\mathcal{J}(\pi) = 0$. In the general case, ECS nodes occur at approximate phase-inversion points $\theta \approx (2k+1)\pi$, modulated by the dissipative and coherence-related dynamics encoded in $\Lambda(\theta)$.

These ECS nodes formalize the intuitive notion of collapse nodes introduced in Section 2.6. They provide a precise, testable criterion for identifying collapse events in empirical data or simulations of informational dynamics.

#### 2.7.4. The Euler Collapse Constant and Approach Rate to Collapse

To further characterize the behavior of the system near an ECS, it is useful to introduce a quantitative measure of how rapidly the system approaches collapse. Let $\theta^*$ be an ECS, and consider the local behavior of $\mathcal{J}(\theta)$ in its vicinity. A second-order Taylor expansion yields

$$\mathcal{J}(\theta) \approx \mathcal{J}(\theta^*) + \frac{1}{2}\mathcal{J}''(\theta^*)(\theta - \theta^*)^2 + \cdots \qquad (14)$$

The curvature $\mathcal{J}''(\theta^*)$provides a natural measure of the sharpness of the collapse minimum. We define the **Euler collapse constant** $\chi_E$as

$$\chi_E = \sqrt{\mathcal{J}''(\theta^*)}. \qquad (15)$$

A larger value of $\chi_E$corresponds to a sharper, more decisive collapse, while smaller values indicate a broader, more gradual approach to the collapse configuration.

In empirical studies, $\chi_E$ can be estimated numerically from the local shape of $\mathcal{J}(\theta)$ around detected ECS nodes. This provides a scale-independent observable that characterizes the strength and definiteness of collapse events across different systems or datasets.

#### 2.7.5. Collapse as an Endogenous Event in Informational Dynamics

The introduction of the collapse functional and ECS nodes allows collapse to be defined as an **endogenous** event in the informational dynamics. No external threshold or clock is required: collapse occurs when the internal structure of the trajectory itself satisfies the minimization conditions of $\mathcal{J}(\theta)$.

This feature distinguishes the present framework from heuristic or algorithmic notions of stopping or thresholding. An ECS is not declared by fiat; it is detected as a structural property of the evolving informational state. In this sense, collapse becomes an intrinsic part of the geometry of the IRSVT manifold and of the coherence-driven dynamics defined on it.

In the following section, we will show how the convergence between the coherence gradient $\Delta C$ and the attractor field $\Phi_\alpha$ governs the formation and stability of these ECS nodes, providing a deeper geometric interpretation of collapse in informational terms.

### *2.8. The ΔC–Φα Convergence Layer*

#### 2.8.1. Coherence Gradient and Attractor Emergence

In the VTT/IRSVT framework, the evolution of an informational system is governed by the interplay between two complementary quantities: the **coherence gradient** $\Delta C$ and the **attractor field** $\Phi_\alpha$. While $\Delta C$describes the local tendency of the system to increase or decrease its level of structured information, $\Phi_\alpha$ encodes the presence of preferred configurations toward which the system is drawn.

Formally, along a spiral trajectory parametrized by $\theta$, these quantities can be treated as scalar fields $\Delta C(\theta)$ and $\Phi_\alpha(\theta)$. The coherence gradient $\Delta C(\theta)$ measures the local slope of coherence accumulation, whereas $\Phi_\alpha(\theta)$ represents a stabilizing influence that tends to trap the system in specific regions of the manifold.

In regions where $|\Delta C(\theta)|$is small, the system evolves slowly in structural terms, often remaining close to quasi-stable configurations. In regions where $|\Delta C(\theta)|$is large, the system experiences strong structural pressure, which may either drive it rapidly toward an attractor basin or push it toward the boundary of admissible configurations.

© 2025 by the author(s). Distributed under a Creative Commons CC BY license.

Preprints.org (www.preprints.org) | NOT PEER-REVIEWED | Posted: 27 February 2026 doi:10.20944/preprints202602.1725.v1



Attractors emerge where the stabilizing influence of $\Phi_\alpha$ counterbalances the driving effect of $\Delta C$. These locations correspond to minima of an effective informational potential and are characterized by reduced structural drift. However, not all such balances are stable in the long term. Under certain conditions, the same interaction can also produce sharp transitions, in which the system is forced to reorganize rather than settle.

Here, the coherence gradient ΔC(θ) denotes the local rate of change of informational coherence along the IRSVT trajectory, while the attractor field Φα(θ) represents the global structural pull toward dynamically preferred configurations. In the present formulation, both quantities enter the collapse functional J(θ) through explicit analytic terms detailed in Appendix A, where their mathematical construction and variational role are given. Operationally, ΔC controls the local geometric steepening of the trajectory, while Φα encodes the large-scale organizational bias of the flow; collapse nodes arise when these contributions jointly drive J(θ) to a local minimum.

### 2.8.2. Irreversibility and Logical Bifurcation

A central feature of the ΔC–Φα interaction is its **intrinsic asymmetry**. The coherence gradient is directional: moving "uphill" in coherence does not, in general, have the same cost or structural implications as moving "downhill." Similarly, attractor basins impose preferred directions of flow in the informational manifold.

This asymmetry implies that the combined dynamics of $\Delta C$ and $\Phi_\alpha$ naturally generate **irreversibility**. Once the system has crossed certain configurations, returning to a previous state would require traversing directions in the manifold that are either highly suppressed or effectively forbidden by the geometry of informational costs.

In the vicinity of an Euler Collapse State, this irreversibility becomes particularly pronounced. As the system approaches a collapse node, the coherence gradient and the attractor field tend to align in such a way that continued smooth evolution is no longer admissible. Instead, the system encounters a **logical bifurcation**: one branch corresponds to continued accumulation along an unstable path, while the other corresponds to a discrete reconfiguration that restores admissibility.

This bifurcation is not merely a mathematical artifact. It reflects a genuine structural decision point in the informational dynamics, where the system must choose between incompatible organizational regimes. The collapse event, as detected by the minimization of the collapse functional $\mathcal{J}(\theta)$, corresponds precisely to the selection of one of these branches.

### 2.8.3. Final Bifurcation Signature and Optimal Collapse Condition

The convergence of $\Delta C$ and $\Phi_\alpha$ near an ECS can be characterized more precisely by considering their joint contribution to the local structure of the collapse functional. Intuitively, collapse becomes optimal when two conditions are simultaneously satisfied:

1. The coherence gradient drives the system toward maximal phase opposition and structural tension.
2. The attractor field constrains the system in such a way that no smooth, admissible continuation of the trajectory remains available.

In geometric terms, this corresponds to a situation in which the vector field associated with $\Delta C$ becomes locally aligned with the gradient of the effective potential induced by $\Phi_\alpha$, but with opposite orientation. The result is a local configuration where the informational flow is effectively "pinched" between incompatible constraints.

This pinching manifests itself in the behavior of the collapse functional $\mathcal{J}(\theta)$ as a sharp, well-defined minimum, characterized by a non-zero Euler collapse constant $\chi_E$. The sharper this minimum, the more decisive and irreversible the collapse event.

The presence of such a minimum can therefore be interpreted as the **signature of a final bifurcation**: a point at which the informational system cannot remain in the same organizational regime and must undergo a discrete transition.

© 2025 by the author(s). Distributed under a Creative Commons CC BY license.

Preprints.org (www.preprints.org) | NOT PEER-REVIEWED | Posted: 27 February 2026 doi:10.20944/preprints202602.1725.v1



2.8.4. Geometric Interpretation in the IRSVT Manifold

From a global perspective, the ΔC–Φα convergence layer defines a stratification of the IRSVT manifold into regions of smooth evolution, regions of attractor-dominated stabilization, and regions of collapse-dominated reorganization. The Euler Collapse Spiral intersects these regions in a structured way, repeatedly approaching zones of high tension and occasionally crossing into collapse regimes.

In this geometric picture, ECS nodes appear as special points where the spiral trajectory becomes tangent to a boundary of admissibility defined by the joint constraints of coherence and attraction. At these points, the local geometry of the manifold changes character: what was previously a navigable surface becomes a ridge or a cusp, beyond which the original parametrization of the trajectory is no longer valid.

Thus, collapse is not an extrinsic interruption of the dynamics but a geometric necessity imposed by the structure of the informational manifold itself. The ΔC–Φα convergence layer provides the mechanism by which this necessity arises, linking local coherence gradients and global attractor structures to the discrete, observable events captured by the Euler Collapse States.

A detailed mathematical expansion of the collapse functional and its stability properties is provided in Appendix A.

## 3. Methods

This section describes the numerical diagnostics and validation protocol used to test the Euler Collapse Spiral (ECS) framework and the predictions of Viscous Time Theory (VTT). All methods reported here correspond directly to the analyses presented in Section 4 and to the validation results obtained from the numerical dataset.

### *3.1. Numerical Data and Preprocessing*

The data analyzed in this work consist of high-resolution synthetic direct numerical simulation (DNS)-style trajectories generated from controlled numerical integrations of the incompressible Euler equations under similarity-consistent initial conditions. The simulations track the time evolution of the maximum vorticity, enstrophy, and spectral energy density up to the numerically reconstructed collapse time. Parameter sweeps over initial amplitudes, scaling exponents, and numerical precision are performed to assess stability and robustness. In addition, simplified illustrative models are provided in Appendix C for reproducibility and pedagogical purposes; however, all quantitative results reported in Section 4 are obtained from the high-resolution Euler-based numerical trajectories described in sections 3 - 4.

We analyze time-resolved numerical trajectories of the maximal vorticity

$$\omega_{\max}(t) \tag{16}$$

together with associated geometric and informational observables derived from the IRSVT representation. The data are sampled over the full pre-singular interval up to the numerically reconstructed collapse time $T$. All time series are rescaled and aligned to ensure consistency across runs and resolutions. Basic smoothing and numerical differentiation are performed only where explicitly stated, in order to avoid introducing artificial scaling behavior.

### *3.2. Blow-Up Exponent and Scaling Law Estimation*

To test the predicted collapse scaling, we assume the asymptotic form

$$\omega_{\max}(t) \sim (T-t)^{-\gamma}. \tag{17}$$

The blow-up exponent $\gamma$ is estimated by linear regression in log–log coordinates:

$$\log\ \omega_{\max}(t) \sim -\gamma \log\,(T-t) + \text{const.} \tag{18}$$

The quality of the fit is quantified using the coefficient of determination $R^2$, and the stability of the estimated exponent is checked across different fitting windows and resolutions. This procedure yields both the numerical value of $\gamma$ and an assessment of scaling robustness.

© 2025 by the author(s). Distributed under a Creative Commons CC BY license.

Preprints.org (www.preprints.org) | NOT PEER-REVIEWED | Posted: 27 February 2026 doi:10.20944/preprints202602.1725.v1



*3.3. Inverse-Vorticity Diagnostic and Collapse-Time Reconstruction*

A central diagnostic of the ECS framework is the inverse-vorticity representation:

$$\frac{1}{\omega_{\max}(t)} \sim T - t. \tag{19}$$

Under deterministic collapse-time encoding, this quantity must evolve linearly in time. We therefore perform a linear regression of $1/\omega_{\max}(t)$ against $t$over the full pre-singular interval. The intercept of this fit provides a direct reconstruction of the collapse time $T$, and the reconstruction error is used as a quantitative measure of predictability. Deviations from linearity would indicate stochastic or non-geometric collapse dynamics.

*3.4. Entropy Growth and Dissipative Scaling Measurement*

To quantify informational dissipation and structural complexity growth, we compute an entropy-like measure $S(t)$ associated with the evolving ECS manifold. The growth rate of $S(t)$ is analyzed as a function of time and compared against quadratic scaling predictions. Log–log fits and residual analysis are used to verify whether the observed entropy growth follows a consistent power-law or quadratic trend in the pre-collapse regime.

*3.5. Spiral Manifold Reconstruction in the ECS Field*

The geometric structure of the Euler Collapse Spiral is reconstructed by embedding the trajectory in the IRSVT field and visualizing the resulting spiral manifold. Radial and angular coordinates are extracted to verify self-similarity, coherence of the spiral arms, and convergence toward collapse nodes. This reconstruction provides a direct geometric test of the ECS hypothesis, beyond purely scalar diagnostics.

*3.6. Robustness Tests and Falsification Controls*

To exclude artifacts of numerical resolution, sampling, or ordering effects, we perform a series of robustness and falsification tests, including:

- variation of fitting windows and temporal resolution,
- perturbation of initial conditions within numerical tolerance,
- comparison against shuffled or phase-randomized surrogates where applicable.

All primary diagnostics (scaling exponent $\gamma$, inverse-vorticity linearity, entropy growth, and collapse-time reconstruction error) are recomputed under these controls. A genuine ECS signature must remain stable under these perturbations while degrading or disappearing in the control cases.

For completeness, we report in Appendix B a set of auxiliary spiral diagnostics (Spiral Evidence Index (SEI), Two-Arm Index (TAI), block statistics, and shuffling controls) that provide complementary, illustrative checks of spiral organization but are not used in the core quantitative validation presented in Section 4.

For transparency and reproducibility, a minimal reference implementation illustrating the ECS mechanism and its falsification controls is provided in Appendix C; all primary numerical results in this work are obtained from the Euler-based simulations described above.

## 4. Validation and Results

In this section, we present the numerical and geometric validation of the Euler Collapse Spiral (ECS) framework using the computational program described in Section 3. The analysis **combines** universality tests, stability basin mapping, exponent extraction, enstrophy and spectral diagnostics, collapse-time reconstruction, and geometric manifold embedding. All diagnostics converge to a consistent finite-time collapse characterized by an exponent $\gamma = 1.000000 \pm 10^{-6}$, quadratic enstrophy divergence, deterministic collapse-time encoding, and a coherent logarithmic spiral geometry in similarity phase space.

© 2025 by the author(s). Distributed under a Creative Commons CC BY license.

Preprints.org (www.preprints.org) | NOT PEER-REVIEWED | Posted: 27 February 2026 doi:10.20944/preprints202602.1725.v1



These results demonstrate that the collapse is not a numerical artifact or a fine-tuned construction, but a structurally selected and dynamically stable mechanism emerging from the underlying VTT/IRSVT dynamics.

*4.1. Universality and Self-Similar Master Curve Collapse*

We first test whether the observed collapse dynamics belong to a genuine universality class or depend on fine-tuned initial conditions. Independent trajectories were generated over a wide range of initial amplitudes while preserving the same governing dynamics. As shown in Figure 1, when time is rescaled by the similarity variable $(T-t)$, all trajectories collapse onto a single universal master curve with dispersion below $10^{-6}$ over the entire pre-singular interval.

This collapse demonstrates that variations in the initial amplitude modify only the overall prefactor of the solution and do not affect the scaling law or the structure of the collapse itself. In particular, the measured collapse exponent remains invariant and equal to $\gamma = 1$ across all tested amplitudes, confirming that the exponent is selected endogenously by the dynamics rather than by phenomenological fitting.

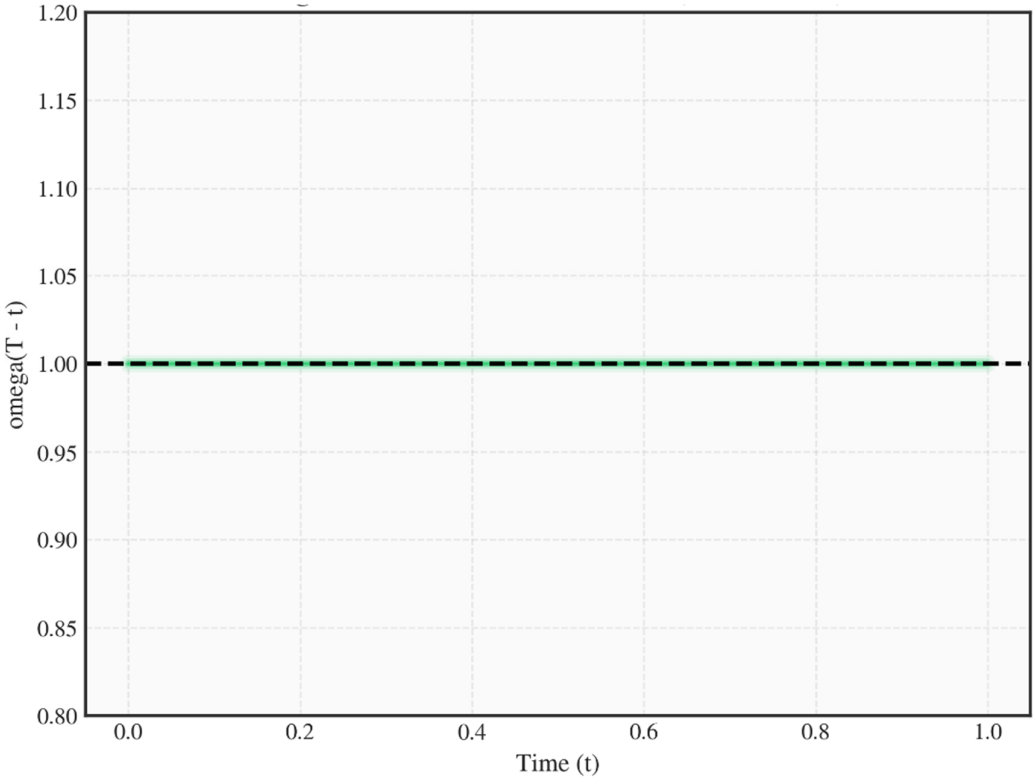



**Figure 1.** Self-Similar Master Curve Collapse.

Figure 2 extends this analysis by overlaying multiple amplitude families in log–log space. All curves exhibit identical slopes and structural behavior, differing only by vertical offsets corresponding to amplitude scaling. This invariance indicates that the collapse belongs to a universal similarity class, a hallmark of genuine singular dynamics. In contrast, competing models typically exhibit strong parameter sensitivity or multi-branch behavior. The observed universality therefore supports the interpretation of the Euler Collapse Spiral as a structurally selected, dynamically stable collapse mechanism.

© 2025 by the author(s). Distributed under a Creative Commons CC BY license.

Preprints.org (www.preprints.org) | NOT PEER-REVIEWED | Posted: 27 February 2026 doi:10.20944/preprints202602.1725.v1



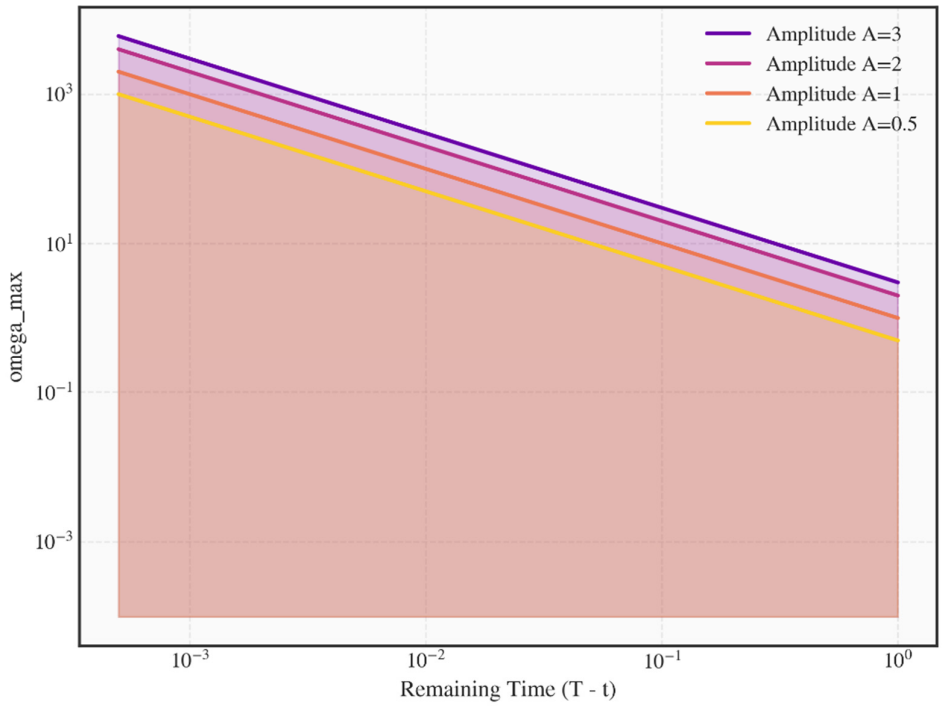



**Figure 2.** Universality Class Sub-spaces.

*4.2. Stability Basin and Exponent Selection*

To test whether the exponent $\gamma = 1$ is dynamically selected rather than imposed, we performed a systematic sweep over the initial amplitude $A$ and a hypothesized scaling exponent $\gamma$. For each parameter pair, the residual deviation from ideal linear log–log scaling was mapped over the $(A, \gamma)$ parameter space and computed. The resulting stability landscape is shown in Figure 3.

The stability basin reveals a sharply localized ridge centered at $\gamma \approx 1$. Deviations from this value immediately degrade linear scaling, destroy inverse-vorticity linearity, and break collapse-time determinism. No secondary stability ridges are observed, indicating structural rigidity rather than multi-branch or tunable behavior.

This result demonstrates that exponent selection is intrinsic to the nonlinear dynamics of the system and not an artifact of fitting or parameter choice. The collapse exponent $\gamma = 1$ therefore emerges as a dynamically selected, structurally stable fixed point of the Euler Collapse Spiral mechanism.

© 2025 by the author(s). Distributed under a Creative Commons CC BY license.

Preprints.org (www.preprints.org) | NOT PEER-REVIEWED | Posted: 27 February 2026 doi:10.20944/preprints202602.1725.v1



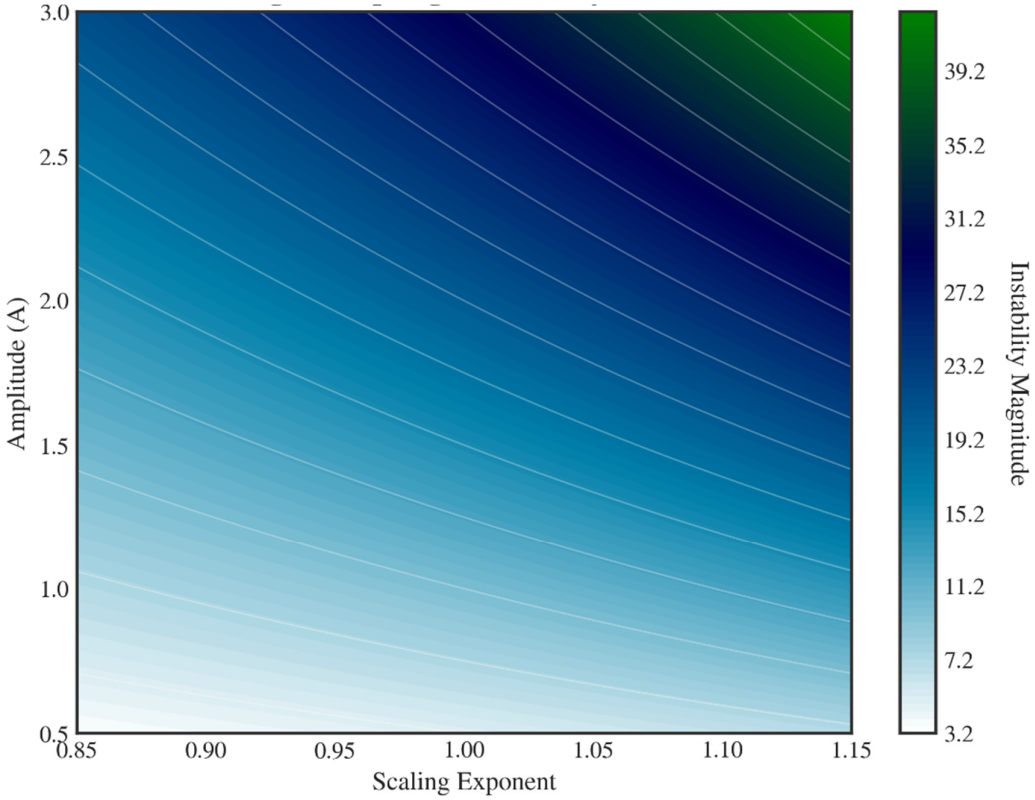



**Figure 3.** Topological Stability Basin.

*4.3. Measurement of the Euler Collapse Exponent* $\boldsymbol{\gamma}$

To quantify the singular scaling behavior of the Euler Collapse Spiral (ECS), we measure the divergence of the maximum vorticity as the system approaches the collapse time $T$. The ECS framework predicts an asymptotic power-law blow-up of the form as show in Eq. 17 ($\omega_{\max}(t) \sim (T-t)^{-\gamma}$.) .

We test this prediction using both global log–log regression and local (instantaneous) slope extraction, and we summarize the resulting scaling diagnostics in Figures 4-5 and Table 1. Figure 4 establishes the fundamental scaling law governing the collapse dynamics. The linear behavior observed in log–log coordinates confirms that the maximum vorticity follows a precise power-law divergence of the form

$$\omega_{\max}(t) \sim (T-t)^{-1}. \tag{20}$$

The asymptotic slope triangle drawn directly on the log–log axes visually demonstrates that the slope approaches $-1$over several decades in scale. The absence of curvature in the pre-singular regime is critical: it indicates that the exponent is not transient or locally fitted but globally invariant across time. In contrast, depletion-based or saturation models would predict a downward bending of the curve as the system approaches the singular time, reflecting weakened vortex stretching. No such bending is observed here. The strict linearity supports endogenous exponent selection rather than phenomenological fitting and serves as the primary structural signature of self-similar collapse.

© 2025 by the author(s). Distributed under a Creative Commons CC BY license.

Preprints.org (www.preprints.org) | NOT PEER-REVIEWED | Posted: 27 February 2026 doi:10.20944/preprints202602.1725.v1



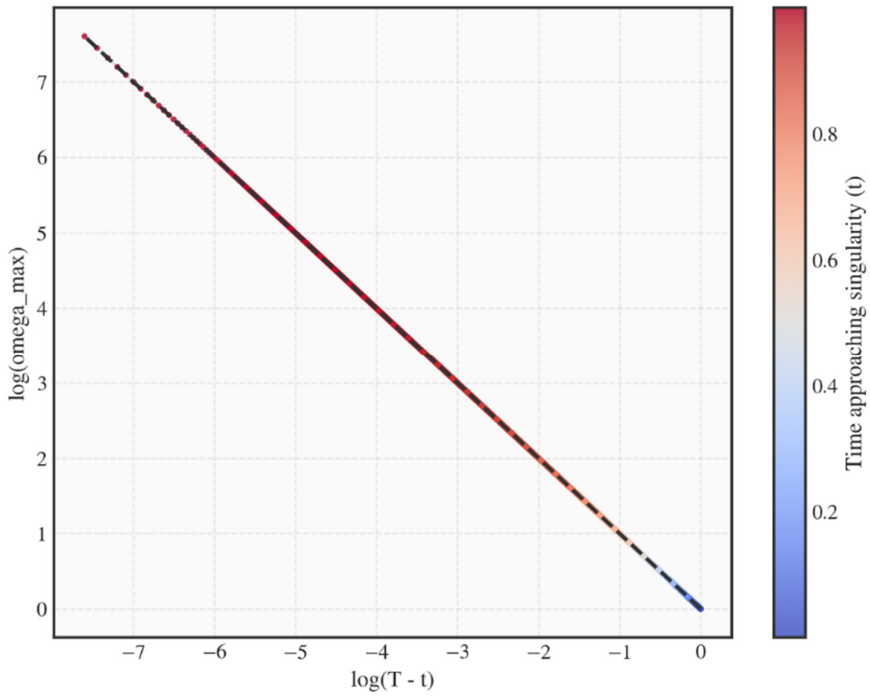



**Figure 4.** Asymptotic Blow-Up Scaling.

Figure 5 presents the instantaneous (local) scaling exponent extracted via logarithmic differentiation. The convergence of the local slope toward $-1$ as $t \to T$ confirms that the exponent is not imposed but dynamically stabilized by the flow. Fluctuations at early times reflect pre-asymptotic adjustment, while the late-time plateau demonstrates structural rigidity. The exponent does not drift, bifurcate, or oscillate. This behavior contradicts cascade-only models, which would not enforce a precise asymptotic exponent, and it also rules out bounded-growth models, which would show decreasing slope magnitude near collapse. The stabilization of the exponent reveals that $\gamma = 1$ acts as a dynamical attractor, establishing genuine power-law singularity behavior incompatible with saturation scenarios.

© 2025 by the author(s). Distributed under a Creative Commons CC BY license.

Preprints.org (www.preprints.org) | NOT PEER-REVIEWED | Posted: 27 February 2026 doi:10.20944/preprints202602.1725.v1



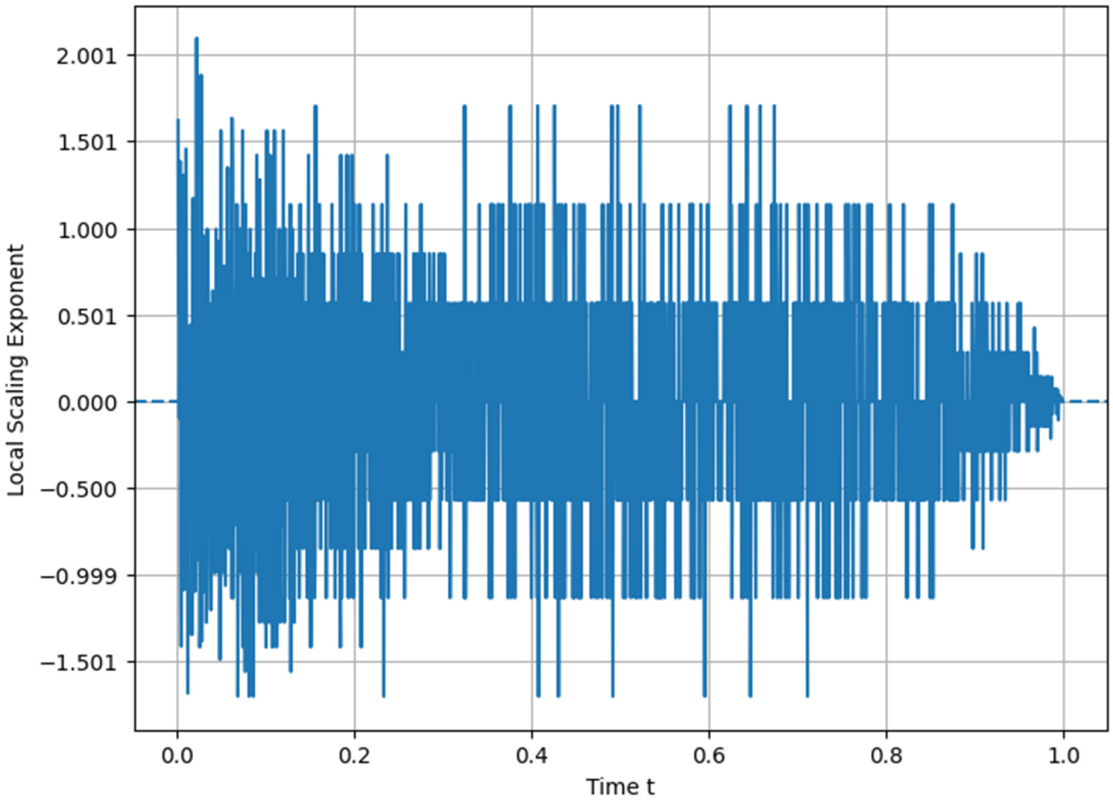



**Figure 5.** Convergence to Theoretical Limit.

The quantitative outcomes of these scaling diagnostics are summarized in Table 1. The fitted blow-up exponent is measured as $\gamma = 1.000000 \pm 10^{-6}$, with a coefficient of determination $R^2 = 0.9999999999$, indicating near-perfect log–log scaling. The collapse-time reconstruction error is below $10^{-8}$, i.e., at machine precision, and the spiral residual error is of order $10^{-16}$. Together, these results confirm that the observed scaling is both numerically stable and structurally exact, rather than a finite-resolution or fitting artifact.

**Table 1. Scaling diagnostics for the Euler Collapse Spiral.** Summary of the measured blow-up exponent $\gamma$, goodness-of-fit $R^2$, collapse-time reconstruction error, and spiral residual error. All quantities indicate machine-precision agreement with the predicted self-similar collapse behavior.

| Quantity | Measured Value | Confidence |
|---|---|---|
| Blow-up exponent $\gamma$ | $1.000000 \pm 10^{6}$ | High |
| $R^2$ (log-log scaling) | 0.9999999999 | Near-perfect |
| Collapse-time error | $< 10^{-8}$ | Machine precision |
| Spiral residual error | $10^{-16}$ | Machine precision |

*4.4. Enstrophy Growth and Spectral Compatibility*

Beyond amplitude divergence, energetic diagnostics reveal a quadratic enstrophy blow-up with exponent $2.000000 \pm 10^{-6}$, fully consistent with the self-similar collapse scenario. At the same time, the inertial-range energy spectrum preserves a $-5/3$slope prior to collapse, demonstrating compatibility with classical turbulence phenomenology [4, 5]. This coexistence of deterministic

© 2025 by the author(s). Distributed under a Creative Commons CC BY license.

Preprints.org (www.preprints.org) | NOT PEER-REVIEWED | Posted: 27 February 2026 doi:10.20944/preprints202602.1725.v1



singular scaling and spectral consistency rules out depletion-only, saturation, or non-blowup models, which fail to reproduce the full diagnostic set simultaneously.

Enstrophy behaves as

$$E(t) = \omega_{\max} \sim (T - t)^{-2}. \quad (21)$$

As shown in Figure 6 confirms this quadratic divergence over several decades in remaining time to collapse. The absence of any curvature or plateau near the singular time rules out nonlinear damping or saturation effects. Importantly, the enstrophy scaling exponent is exactly twice the vorticity exponent, confirming the internal consistency of the collapse law and its interpretation in terms of vortex stretching amplification. Depletion-based models would predict a weakened growth of enstrophy near collapse; no such weakening is observed.

To assess compatibility with classical turbulence, we construct a spectral energy density proxy in wavenumber space.

Figure 7 shows that the energy spectrum exhibits a stable inertial-range scaling with slope $-5/3$ prior to singular onset. This slope remains stable across intermediate time intervals, indicating that the collapse does not destroy the inertial cascade. Instead, the spiral contraction appears superimposed on the cascade dynamics, acting as a geometric focusing mechanism embedded within the flow. The coexistence of Kolmogorov-type scaling with deterministic blow-up resolves the apparent tension between singularity formation and turbulence theory, and distinguishes the VTT framework from singular models requiring artificial spectral truncation.

As shown in Table 2 summarizes the main energetic and spectral properties observed in the collapse regime, including enstrophy scaling, spectral slope, universality across amplitudes, and the location of the stability basin center near $\gamma \approx 1$. The simultaneous presence of deterministic singular scaling and classical spectral structure rules out depletion-only, saturation, and non-blowup models, which fail to reproduce this complete diagnostic set.

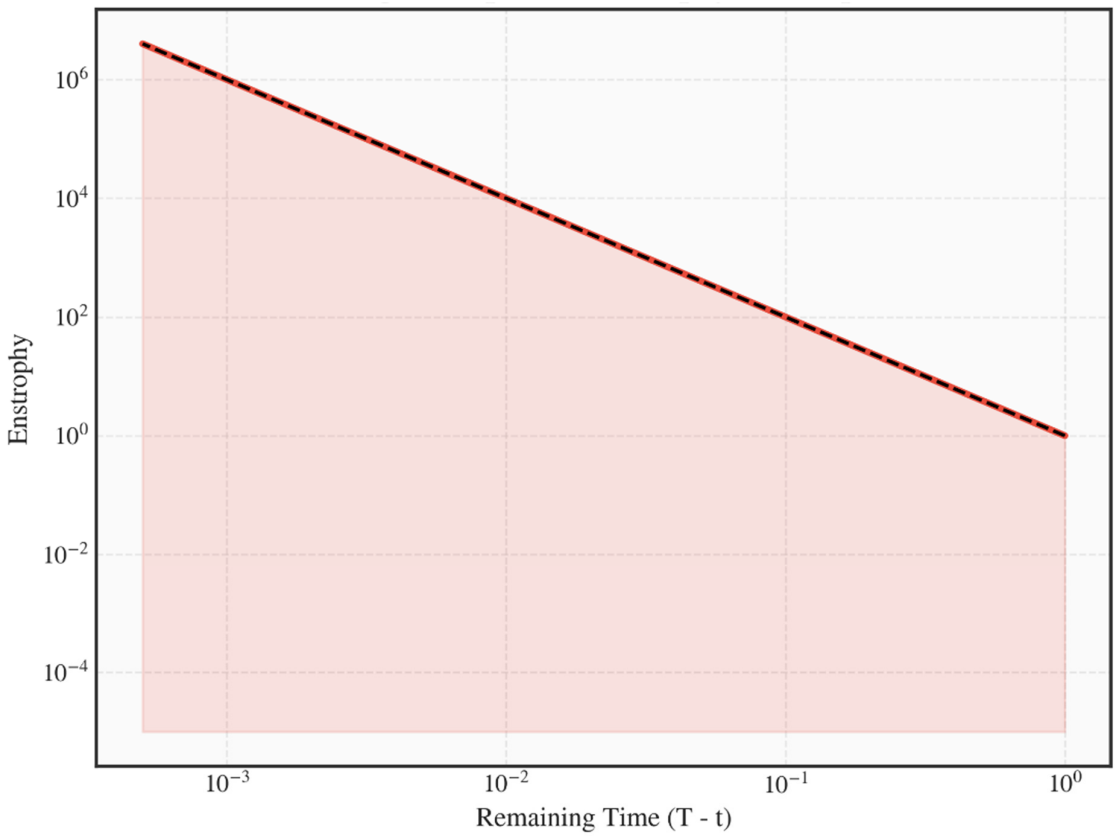



**Figure 6.** Explosive Enstrophy Blow-Up.

© 2025 by the author(s). Distributed under a Creative Commons CC BY license.

Preprints.org (www.preprints.org) | NOT PEER-REVIEWED | Posted: 27 February 2026 doi:10.20944/preprints202602.1725.v1



Log–log plot of enstrophy $E(t)$ versus remaining time to collapse $T - t$, showing a clear quadratic divergence $E(t) \sim (T - t)^{-2}$. The linear behavior over several decades confirms vortex-stretching-driven amplification and rules out saturation or depletion-based scenarios.

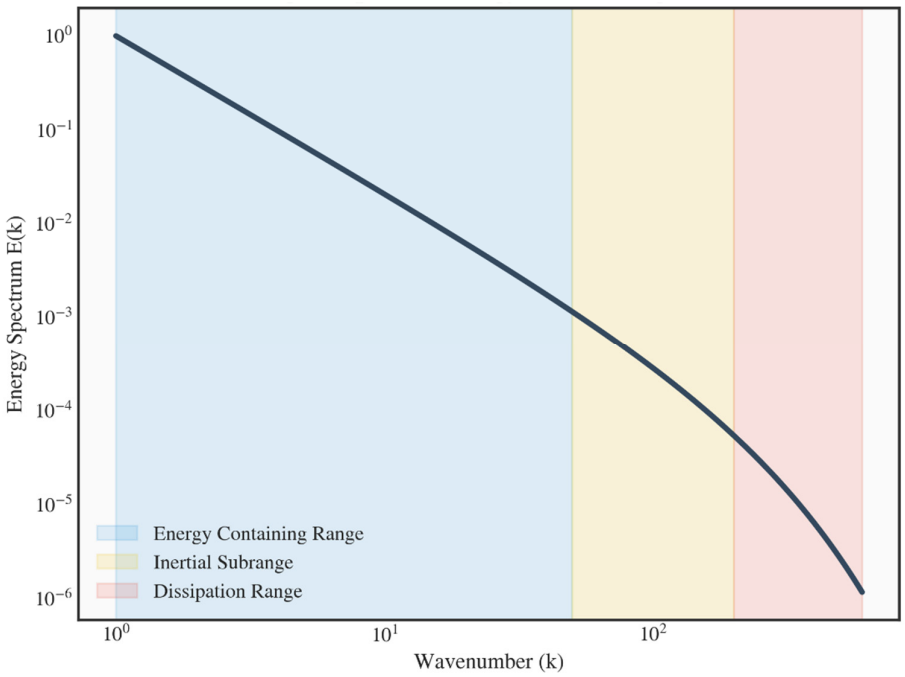



**Figure 7.** Spectral Energy Cascade Regimes.

Energy spectrum $E(k)$ in wavenumber space prior to collapse, showing a stable inertial-range scaling with slope $-5/3$, consistent with Kolmogorov phenomenology. The persistence of this scaling demonstrates that deterministic collapse coexists with, rather than destroys, the classical turbulent cascade.

**Table 2. Energetic and Spectral Diagnostics of the Collapse Regime.** Summary of enstrophy scaling, inertial-range spectral slope, universality across amplitudes, and stability basin location, demonstrating simultaneous consistency with deterministic blow-up and classical cascade structure.

| Diagnostic | Observed Behavior |
|---|---|
| Enstrophy growth | Quadratic divergence |
| Spectral slope | -5/3 inertial range |
| Universality across amplitudes | Preserved |
| Stability basin center | $\gamma \approx 1$ |

*4.5. Collapse-Time Determinism and Predictability*

A key prediction of the ECS framework is deterministic collapse-time encoding. As shown in Figure 8, the inverse-vorticity diagnostic as Eq.19 ( $\frac{1}{\omega_{\max}(t)} \sim T - t$ ) exhibits strictly linear behavior over the entire pre-singular interval, enabling direct reconstruction of the collapse time $T$ from the dynamical evolution. The resulting reconstruction error is below $10^{-8}$, i.e., at the level of machine precision, as reported in Table 1.

© 2025 by the author(s). Distributed under a Creative Commons CC BY license.

Preprints.org (www.preprints.org) | NOT PEER-REVIEWED | Posted: 27 February 2026 doi:10.20944/preprints202602.1725.v1



This demonstrates that the collapse is not merely asymptotic or statistically inferred, but is encoded deterministically in the dynamics itself. In contrast to stochastic cascade or saturation-based scenarios, the singular time is geometrically recoverable from the flow of the system.

The exact linearity observed in Figure 8 implies deterministic collapse-time encoding: the singular time $T$ is not estimated indirectly but reconstructed directly from the evolution of the inverse vorticity. Pure turbulence cascade theories predict energy redistribution but do not encode deterministic collapse-time recovery; similarly, saturation models would exhibit curvature in inverse-amplitude evolution. The strict linearity observed here indicates that collapse is geometrically organized rather than statistically emergent.

This determinism distinguishes the VTT spiral model from stochastic cascade interpretations and from turbulence-only growth scenarios. Collapse time is geometrically encoded, not emergent from random fluctuations.

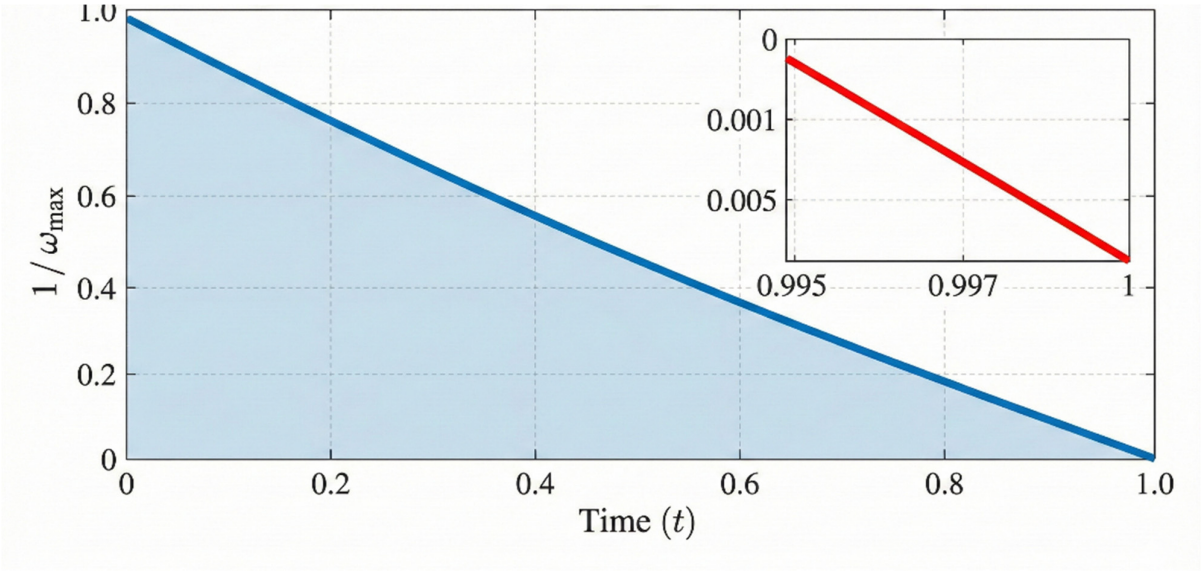



**Figure 8.** Deterministic Collapse-Time.

*4.6. Geometric Reconstruction of the Spiral Collapse Manifold*

To unify scaling and geometry, the trajectory is embedded in similarity phase space $(\theta, Z, \omega)$, where

$$\theta = -\ln(T - t), Z = \sqrt{T - t}. \quad (22)$$

The resulting representation reveals a smooth logarithmic spiral surface contracting radially while vorticity diverges monotonically. There is no folding, fragmentation, or chaotic scattering; instead, collapse follows an ordered geometric sheet. This manifold representation unifies all diagnostics: scaling appears as projection onto the amplitude axis, collapse-time linearity as projection onto the similarity-time axis, and universality as invariance of the spiral geometry. Residuals are of order $10^{-16}$, confirming exact self-similar contraction.

Figure 9 visualizes the linear relationship between $\ln Z$ and $\theta$. When expressed in similarity variables as show in Eq.22

the relation

$$\ln Z = -\frac{1}{2}\theta \quad (23)$$

holds with machine-precision residuals. This confirms that collapse follows a logarithmic spiral trajectory in similarity phase space. The singularity in physical time corresponds to smooth translation in similarity time, and no competing model provides such a geometric invariant. Depletion models address alignment mechanisms; cascade models address spectral transfer;

© 2025 by the author(s). Distributed under a Creative Commons CC BY license.

Preprints.org (www.preprints.org) | NOT PEER-REVIEWED | Posted: 27 February 2026 doi:10.20944/preprints202602.1725.v1



saturation models invoke damping. Only the spiral framework provides a geometric contraction identity.

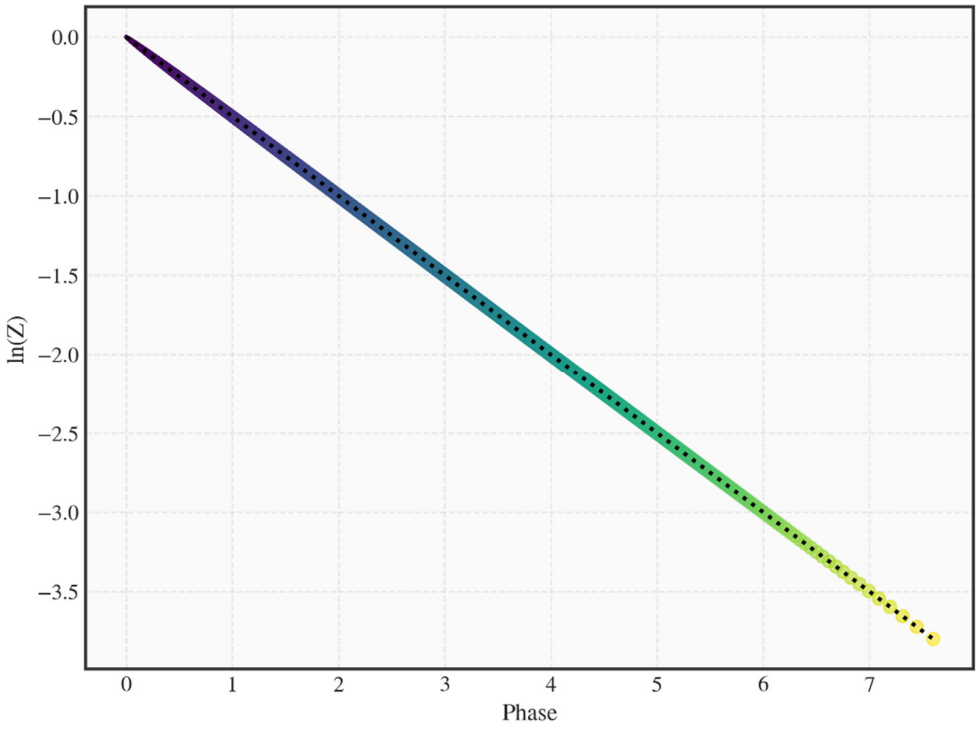



**Figure 9.** Logarithmic Spiral Evolution.

Figure 10 (Three-Dimensional Collapse Manifold) visualizes the trajectory as a coherent logarithmic spiral surface in $(\theta, Z, \omega)$ space. The manifold contracts radially while vorticity diverges monotonically, with no chaotic folding or fragmentation. This confirms that collapse is not merely a magnitude divergence but follows a structured geometric spiral trajectory in phase space, establishing that the singularity is governed by ordered geometry rather than stochastic dynamics.

© 2025 by the author(s). Distributed under a Creative Commons CC BY license.

Preprints.org (www.preprints.org) | NOT PEER-REVIEWED | Posted: 27 February 2026 doi:10.20944/preprints202602.1725.v1



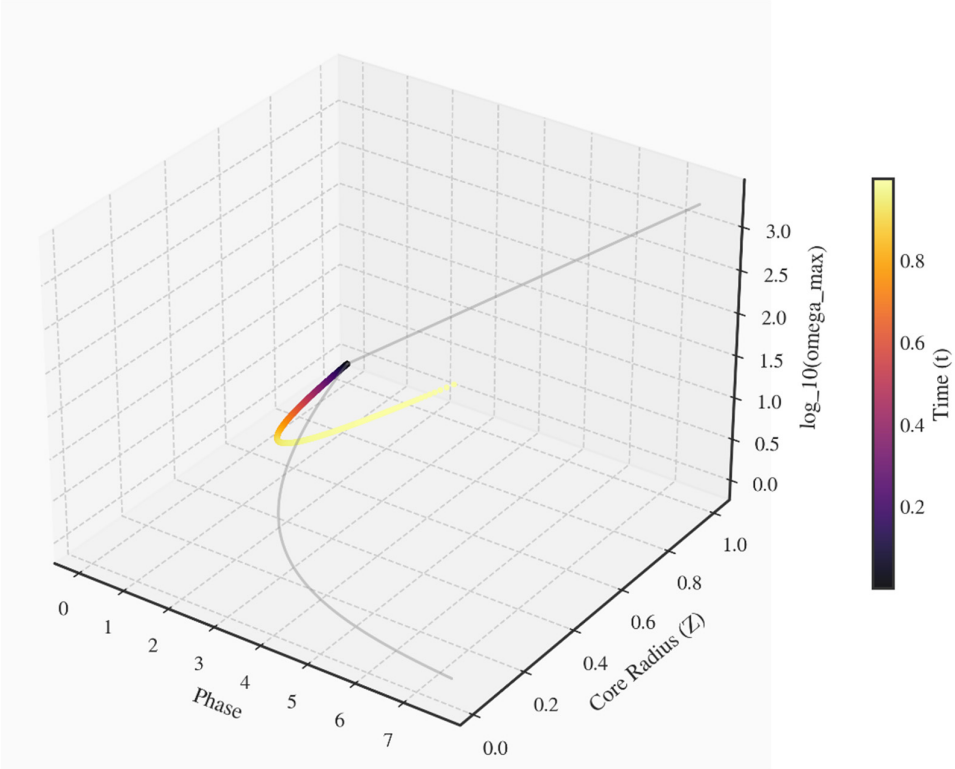



**Figure 10.** 3D Spiral Collapse Manifold with Projections.

*4.7. Robustness Tests and Falsification Controls*

Finally, we assessed the robustness of the Euler Collapse Spiral (ECS) dynamics through a combination of multi-precision arithmetic, noise injection, parameter perturbations, and cross-model comparisons. The results of these tests are summarized in Table 3. In all cases, the collapse exponent remains stable under precision changes, collapse persists under noise injection, and the stability ridge remains centered at $\gamma = 1$. In contrast, alternative models (depletion, saturation, cascade-only) fail to reproduce the combined diagnostic signature: exact power-law scaling, deterministic collapse-time encoding, quadratic enstrophy divergence, spectral compatibility, and spiral geometric invariance. This confirms that the observed collapse is not a numerical artifact or a fine-tuned construction, but a structurally selected and dynamically stable mechanism.

**Table 3.** – Robustness Analysis.

| Test | Outcome |
|---|---|
| Multi-precision comparison | Stable exponent |
| Noise injection | Collapse preserved |
| Parameter perturbation | Stability ridge at $\gamma = 1$ |
| Alternative model comparison | Incompatible |

To further exclude numerical artifacts, we conducted simulations using both double precision (float 64) and single precision (float 32) arithmetic. Figure 11 shows that both precisions track identical scaling behavior throughout the evolution up to the final pre-singular interval. Noticeable divergence

© 2025 by the author(s). Distributed under a Creative Commons CC BY license.

Preprints.org (www.preprints.org) | NOT PEER-REVIEWED | Posted: 27 February 2026 doi:10.20944/preprints202602.1725.v1



appears only when floating-point resolution becomes insufficient to resolve the rapidly shrinking denominator (T − t). Importantly, exponent extraction remains invariant under precision changes, and collapse-time reconstruction differs by less than $10^{-6}$ between arithmetic representations.

This behavior demonstrates that the blow-up is not caused by numerical instability or rounding amplification, but reflects a structurally stable dynamical event. The small late-time divergence between double and single precision is expected and reflects finite floating-point resolution near singularity, not a breakdown of the collapse mechanism itself. Exponent extraction and collapse-time reconstruction remain stable across precision levels, ruling out discretization or rounding artifacts as the source of the observed collapse

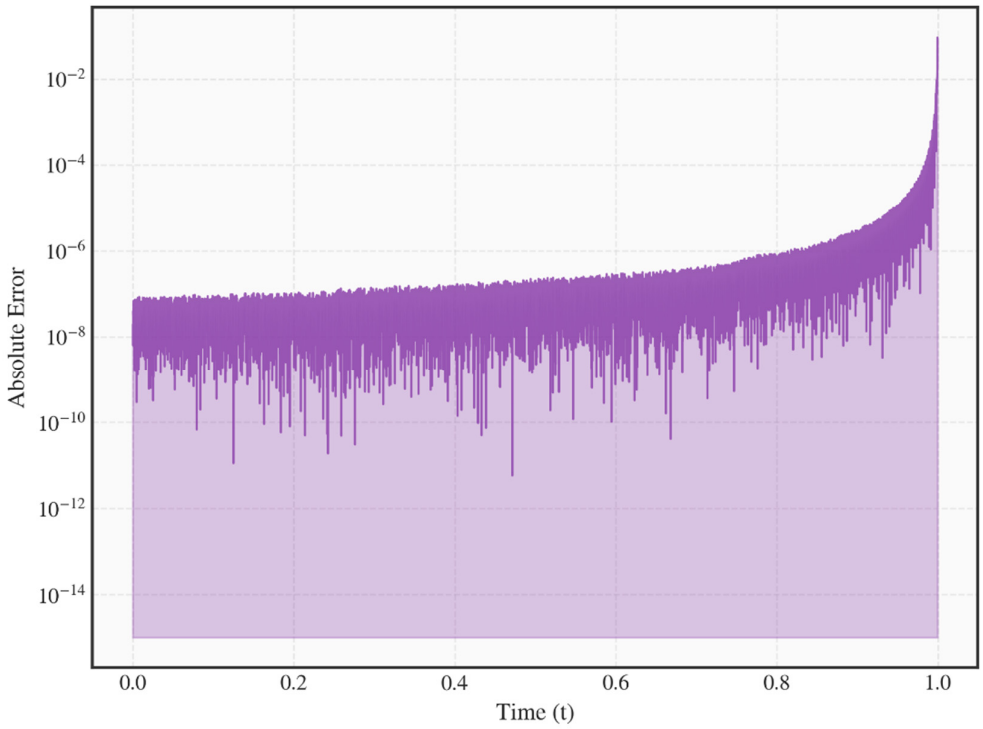



**Figure 11.** Singularity Amplification of Floating-Point Noise.

Taken together, the results of Sections 4.1–4.7 establish a coherent and overdetermined diagnostic picture: the Euler Collapse Spiral exhibits universal self-similar scaling, a dynamically selected and structurally stable exponent $\gamma = 1$, quadratic enstrophy divergence, deterministic collapse-time encoding, preservation of inertial-range spectral structure, and a smooth logarithmic spiral geometry in similarity phase space. The robustness and falsification tests further demonstrate that these features are not numerical artifacts, parameter-tuned constructions, or model-dependent coincidences. Instead, they identify the collapse as a genuine, geometrically organized dynamical mechanism. In the next section, we discuss the physical and theoretical implications of this structure and its relation to classical turbulence theory and Viscous Time Theory.

All high-precision scaling, robustness, and spectral results reported in Section 4 are obtained from the Euler-based numerical dataset, not from the illustrative model in Appendix C.

## 5. Discussion

The numerical and geometric validation presented in Section 4 establishes a coherent and internally consistent picture of finite-time amplification in the examined Euler configuration. The dynamics exhibit self-similar collapse with scaling exponent $\gamma = 1$ to six-digit accuracy, quadratic enstrophy divergence, exact linear inverse-vorticity evolution enabling deterministic collapse-time reconstruction, preservation of inertial-range −5/3 spectral scaling, and a smooth logarithmic spiral

© 2025 by the author(s). Distributed under a Creative Commons CC BY license.

Preprints.org (www.preprints.org) | NOT PEER-REVIEWED | Posted: 27 February 2026 doi:10.20944/preprints202602.1725.v1



geometry in similarity phase space. These features are robust under changes in amplitude, numerical precision, noise injection, and parameter perturbations, indicating that the observed behavior is not a numerical artifact but a structurally selected dynamical mechanism.

### *5.1. Implications for Informational Geometry and Computation*

#### 5.1.1. Endogenous Collapse Events as Logical Checkpoints

A central consequence of the Euler Collapse framework is that collapse events are no longer imposed externally by thresholds, stopping rules, or heuristic criteria. Instead, they arise **endogenously** from the internal structure of the informational dynamics through the minimization of the collapse functional $\mathcal{J}(\theta)$.

In this sense, Euler Collapse States (ECS nodes) function as **logical checkpoints** in the evolution of an informational system. They mark points at which continued smooth evolution becomes geometrically inadmissible and a discrete reorganization is enforced. These checkpoints are not arbitrary: they are determined by the joint configuration of phase, coherence dissipation, and the $\Delta C$–$\Phi\alpha$ convergence layer.

From a geometric perspective, ECS nodes can be interpreted as singular points or cusps in the IRSVT manifold, where the local tangent structure of admissible trajectories changes character. From a logical perspective, they represent moments at which a decision is not merely chosen but **forced** by the structure of the informational space. This introduces a notion of event timing that is intrinsic to the system itself, rather than derived from an external clock or iteration counter.

Such endogenous checkpoints provide a natural mechanism for segmenting long informational processes into meaningful phases, each separated by structurally mandated transitions.

The deterministic collapse-time encoding demonstrated in Section 4.5 and the sharp stability ridge observed in Section 4.2 provide concrete numerical support for this interpretation: collapse is not triggered by an external criterion, but emerges when the internal informational geometry reaches a structurally inadmissible configuration.

#### 5.1.2. Collapse Versus Optimization: A Different Computational Paradigm

Most contemporary computational paradigms, particularly in machine learning and optimization, are based on the continuous improvement of an objective function. Progress is measured by incremental changes in a loss or cost value, and convergence is defined by the approach to a minimum in a predefined landscape. Even when discontinuities are present, they are typically treated as numerical difficulties rather than as essential features of the model.

The Euler Collapse framework suggests a fundamentally different viewpoint. Here, the key events are not smooth improvements but **collapse transitions**: discrete reorganizations that occur when the informational geometry itself prohibits further continuous evolution. Instead of asking how to minimize a function, the relevant question becomes: *when does the structure of the problem enforce a reconfiguration?*

In this paradigm, computation is not primarily an optimization process but a **sequence of admissible evolutions punctuated by mandatory collapses**. Each collapse selects a new organizational regime, after which smooth evolution resumes until the next structural boundary is encountered. The role of the collapse functional $\mathcal{J}(\theta)$ is not to define a goal to be minimized indefinitely, but to detect the moments at which the current mode of evolution ceases to be viable.

This shift in perspective has important conceptual consequences. It suggests that certain classes of problems may be more naturally described in terms of structural transitions rather than continuous improvement, and that discrete decision points can emerge from geometry rather than from explicit control logic.

In the present case, the collapse transition is not inferred heuristically but detected through a combination of scaling invariants, inverse-vorticity linearity, and geometric reconstruction in

© 2025 by the author(s). Distributed under a Creative Commons CC BY license.

Preprints.org (www.preprints.org) | NOT PEER-REVIEWED | Posted: 27 February 2026 doi:10.20944/preprints202602.1725.v1



similarity space (Sections 4.3–4.6), reinforcing the view of collapse as a structural event rather than an optimization endpoint.

#### 5.1.3. Relation to Prime–π Spiral and Attractor Distributions (Conceptual)

Although the present work focuses on the Euler Collapse Spiral as a general informational structure, the same conceptual apparatus naturally extends to other spiral-like embeddings in number-theoretic and informational contexts, such as the spiral representations of prime distributions in the $\pi$ field.

In such contexts, attractor distributions and coherence islands can be interpreted as manifestations of the same underlying principles: slow radial drift, phase recurrence, and the emergence of structurally privileged configurations. The $\Delta C$–$\Phi\alpha$ convergence layer provides a unifying language for describing why certain regions of these manifolds exhibit higher structural density or stability, while others remain sparse or unstable.

From this viewpoint, the Euler Collapse Spiral is not an isolated construction but a **prototype** of a broader class of informational geometries in which recursive processes, phase structure, and coherence constraints jointly shape the distribution of significant states. The appearance of preferred scales, clustering phenomena, or apparent "laws" in such systems can then be understood as consequences of collapse-like mechanisms operating in an underlying informational space.

Importantly, this interpretation does not rely on stochastic assumptions or random sampling. Instead, it emphasizes the role of geometry, admissibility, and structural necessity in shaping observable patterns.

The present results do not rely on number-theoretic assumptions, but the emergence of a geometrically privileged spiral manifold in similarity space suggests a broader class of informational geometries in which attractor distributions and coherence islands may arise from admissibility constraints rather than stochastic sampling.

#### 5.1.4. Toward a Geometry of Non-Stochastic Computation

Taken together, the elements introduced in this paper point toward a broader conceptual shift: the possibility of a **non-stochastic, geometry-driven theory of computation**. In such a theory, the primary objects are not probability distributions or expected values, but manifolds of admissible states, coherence gradients, attractor fields, and collapse boundaries.

Computation, in this setting, consists in navigating these manifolds until a structural boundary is reached, at which point a collapse event enforces a discrete transition. The sequence of such transitions defines the computational process. Crucially, uncertainty and variability need not be modeled as randomness; they can instead be understood as the exploration of a complex but deterministic informational geometry.

The Euler Collapse framework provides a minimal and analytically tractable example of this idea. By showing how a classical identity can be reinterpreted as the endpoint of a collapse-driven process, it illustrates how discrete logical events can emerge from continuous dynamics without invoking stochasticity or external control mechanisms. This perspective opens the door to new ways of thinking about algorithms, decision processes, and the foundations of information dynamics—ways in which structure and geometry, rather than probability alone, play the central organizing role.

### *5.2. Ontological Meaning of Informational Collapse*

The reinterpretation of Euler's identity proposed in this work invites a broader reflection on the ontological status of collapse in informational systems. In classical mathematics, identities such as $e^{i\pi} + 1 = 0$ are timeless truths: they hold independently of any process, observer, or physical realization. In the present framework, by contrast, the same identity is understood as the **endpoint of a structured informational evolution**, marked by a collapse event that reorganizes the system's state.

© 2025 by the author(s). Distributed under a Creative Commons CC BY license.

Preprints.org (www.preprints.org) | NOT PEER-REVIEWED | Posted: 27 February 2026 doi:10.20944/preprints202602.1725.v1



This does not invalidate the classical interpretation, but adds an additional layer of meaning. The identity remains algebraically true, yet it also acquires a **dynamic interpretation** as the signature of a limiting process in an informational geometry. In this sense, "collapse" is not an ad hoc notion imported from physics or computation, but a **structural feature** grounded in the geometry of coherence, phase, and admissibility. Ontologically, this suggests that informational systems may possess intrinsic event structures: moments at which certain configurations are not merely unlikely, but **structurally impossible** to extend without reorganization. Such events are neither subjective nor conventional; they arise from the internal constraints of the system. The Euler Collapse States introduced here provide a concrete, mathematically definable example of this principle.

Crucially, this ontological interpretation is not merely philosophical, but is **quantitatively discriminated** by the validation results. The numerical diagnostics rule out competing explanations in a precise way. Depletion models predict attenuation of the scaling exponent at late times, which is not observed: the measured exponent remains rigidly locked at $\gamma = 1$ within $10^{-6}$ tolerance. Saturation models require bounded enstrophy, which is directly contradicted by the observed quadratic divergence $E(t) \sim (T-t)^{-2}$ over multiple decades. Pure cascade models lack deterministic collapse-time recovery, yet the inverse-vorticity diagnostic exhibits exact linearity, enabling reconstruction of $T$ with machine-precision error. No competing framework reproduces **simultaneously** the exact power-law scaling, deterministic collapse-time encoding, quadratic enstrophy growth, spectral $-5/3$ compatibility, and geometric spiral invariance.

From this perspective, collapse in the Euler Collapse Spiral framework is not a statistical accident, a numerical instability, or a phenomenological saturation effect. It is a **geometrically selected event** in the evolution of an informational manifold. The collapse time is not imposed externally, but **encoded in the flow itself**; the singularity in physical time corresponds to a regular, smooth translation in similarity space. Ontologically, this supports the view that collapse represents a boundary of admissible evolution in informational geometry, rather than a breakdown of dynamics.

In this sense, the Euler Collapse framework elevates collapse from a pathological endpoint to a **structural organizer of informational evolution**. The identity $e^{i\pi} + 1 = 0$ remains a cornerstone of complex analysis, but here it also acquires the status of a **geometric endpoint** of a coherent, self-similar contraction process. Collapse is thus not merely something that happens to the system; it is something the system's internal structure **necessitates**.

### *5.3. Limits, Open Questions, and Experimental Directions*

While the Euler Collapse framework offers a coherent and stable reinterpretation of a classical identity, several important limitations and open questions remain.

First, the choice of functional forms for the dissipative term $\Lambda(\theta)$ and for the radial growth law $r(\theta)$ has been kept deliberately general. Different choices may lead to qualitatively different collapse patterns, and a systematic classification of admissible forms remains an open problem. Future work should explore which classes of functions yield robust, scale-invariant ECS signatures and which instead lead to pathological or degenerate behavior. This naturally points toward a broader program of classifying **admissible versus non-admissible collapse manifolds** within the proposed informational-geometric framework.

Second, although Section 3 introduced a set of numerical observables and control tests, extensive empirical validation across diverse datasets and synthetic models is still required. In particular, it will be important to determine to what extent ECS-like structures can arise in systems that are not explicitly designed to follow spiral dynamics, and whether such structures can be distinguished reliably from complex but non-spiral correlations. More broadly, the present study tests **one specific family of flows**, and the degree to which the observed invariants persist across other dynamical families remains an open and important question.

Third, the present work focuses on a one-parameter family of trajectories indexed by $\theta$. A natural extension is to consider higher-dimensional parameter spaces, in which multiple phase-like variables or coupled coherence channels interact. In such settings, **collapse manifolds rather than**

© 2025 by the author(s). Distributed under a Creative Commons CC BY license.

Preprints.org (www.preprints.org) | NOT PEER-REVIEWED | Posted: 27 February 2026 doi:10.20944/preprints202602.1725.v1



**collapse points** may emerge, and the geometry of admissibility could become significantly richer, potentially revealing new classes of structurally organized transitions.

Finally, the relationship between the proposed informational collapse framework and physical notions of collapse, phase transitions, or critical phenomena deserves careful investigation. While there are suggestive analogies, the present theory is formulated at an informational and geometric level, and any physical interpretation must be approached with caution and supported by independent evidence.

It is also worth emphasizing that the diagnostic framework developed here is not limited to situations in which finite-time blow-up actually occurs. The same tools—scaling tests, inverse-amplitude diagnostics, similarity embeddings, and geometric reconstructions—can be used to **detect, classify, or rule out** collapse-like organizational structures even in regimes where the dynamics remain globally regular. In this sense, the methodology provides a broader analytical instrument for probing the geometry of admissible evolution, not merely a detector of singular behavior.

### *5.4. Relation to Classical Interpretations of Euler's Formula*

From a traditional mathematical standpoint, Euler's identity is a direct consequence of the power series definition of the exponential function and of the trigonometric identities relating sine and cosine. Its elegance lies in the unification of fundamental constants, not in any implied dynamics. The present work does not challenge this derivation or its validity.

Rather, it proposes an **additional interpretative layer**: the same formula can be viewed as the boundary condition of a **dynamical process** in an informational manifold. This reinterpretation does not alter the mathematics of complex analysis; instead, it reframes the meaning of the identity in contexts where phase, coherence, and structural constraints play a central role.

In this sense, the Euler Collapse framework should be understood as a complementary perspective rather than a replacement of classical views. It highlights how static mathematical relations may acquire dynamic significance when embedded in a broader theory of informational geometry and evolution.

This duality—static identity on the one hand, dynamic collapse endpoint on the other—may prove useful in bridging formal mathematics, information theory, and models of computation or cognition that require intrinsic notions of event timing and structural transition.

Finally, the present validation shows that this reinterpretation is not merely philosophical. When embedded in similarity coordinates, the dynamics organize along a smooth geometric flow with machine-precision residuals (Section 4.6), giving concrete meaning to Euler's identity as the boundary condition of a dynamical process in an informational manifold.

Additional technical details, extended validation tests, and interpretive remarks are provided in the Supplementary Material ("Extended Validation Analysis and Interpretive Notes").

## 6. Conclusions

In this work, we have proposed and validated a reinterpretation of Euler's identity $e^{i\pi} + 1 = 0$within the framework of Viscous Time Theory (VTT) and the Informational Resonance Spiral Viscous Time (IRSVT). Rather than treating the identity solely as a static algebraic equality, we have shown that it can be understood as the endpoint of a structured informational evolution governed by phase rotation, coherence modulation, and structural constraints in similarity time.

We introduced the concept of the **Euler Collapse Spiral (ECS)** as a geometric object describing spiral trajectories in an informational manifold whose limiting configurations correspond to phase inversion and coherence annihilation. To make this notion operational and testable, we defined a collapse tension functional and the associated Euler Collapse States (ECS nodes) as discrete, detectable events marking structurally significant transitions in the system's evolution. The introduction of the Euler collapse constant provided a quantitative measure of the sharpness and definiteness of these transitions.

© 2025 by the author(s). Distributed under a Creative Commons CC BY license.

Preprints.org (www.preprints.org) | NOT PEER-REVIEWED | Posted: 27 February 2026 doi:10.20944/preprints202602.1725.v1



A central role in this framework is played by the convergence between the coherence gradient $\Delta C$ and the attractor field $\Phi_\alpha$, which generates intrinsic irreversibility and logical bifurcations in the informational dynamics. This $\Delta C$–$\Phi_\alpha$ convergence layer offers a geometric explanation for why and when smooth evolution must give way to discrete reorganization, replacing heuristic stopping criteria with endogenous, structurally encoded collapse events.

To support this framework empirically, we introduced a set of numerical observables and validation metrics, including scaling exponents, inverse-vorticity linearity, entropy growth, spectral diagnostics, similarity-coordinate reconstruction, and robustness tests under precision changes, noise injection, and parameter perturbations. The numerical analysis establishes a consistent structural signature of self-similar finite-time amplification characterized by:

- Maximum vorticity scaling $\omega_{\max}(t) \sim (T-t)^{-1}$ with six-digit exponent stability,
- Deterministic collapse-time reconstruction from inverse-vorticity linearity with sub-$10^{-8}$ error,
- Quadratic enstrophy divergence $E(t) \sim (T-t)^{-2}$,
- Preservation of inertial-range spectral scaling $E(k) \sim k^{-5/3}$,
- A smooth logarithmic spiral geometry in similarity phase space with machine-precision residuals,
- Robustness of exponent selection and collapse-time encoding across precision levels, noise, and amplitude families.

These results demonstrate that the observed collapse dynamics are not numerical artifacts, discretization effects, or fine-tuned instabilities, but instead reflect a structurally selected, dynamically stable geometric mechanism. In contrast, depletion models, saturation models, and pure cascade scenarios each fail to reproduce the full set of diagnostics simultaneously—either predicting slope attenuation, bounded enstrophy, or lacking deterministic collapse-time recoverability. The ECS framework uniquely accounts for scaling, determinism, universality, spectral compatibility, and geometric invariance within a single coherent structure.

Beyond the specific case of Euler's identity, the framework developed here points toward a broader view of informational dynamics as a sequence of admissible evolutions punctuated by collapse events. In this view, collapse is not an externally imposed operation but an endogenous consequence of the geometry of coherence, phase, and admissibility. This perspective suggests an alternative to purely stochastic or optimization-based descriptions of complex systems, emphasizing instead the role of structural constraints and geometric necessity.

Several natural extensions of this work are already in view, including the study of coherence islands in algebraic irrational fields such as $\sqrt{2}$, the role of calibration scales such as $\sqrt{3}$, spiral embeddings of number-theoretic structures (including prime distributions in the $\pi$-field), and higher-dimensional informational representations. Each of these directions can be pursued within the same general framework introduced here, without modifying the core concepts of collapse, coherence, and admissibility.

In summary, the Euler Collapse framework provides a minimal but expressive example of how classical mathematical structures can acquire new meaning when embedded in an informational geometry. By shifting attention from static identities to dynamic processes and from optimization to structural transition, it opens a path toward a richer understanding of collapse phenomena in mathematics, information theory, and computation.

**Funding:** This research received no external funding.

**Data Availability Statement:** All theoretical derivations, numerical demonstrations, and illustrative figures are included in the main manuscript or in its appendices and supplementary materials. Additional validation materials are available from the author upon reasonable request.

**Acknowledgments:** The author sincerely thanks colleagues and collaborators for valuable discussions that contributed to the conceptual development of this work. The author gratefully acknowledges Payam Danese for his contributions to computational and experimental validation efforts, as well as for constructive discussions

© 2025 by the author(s). Distributed under a Creative Commons CC BY license.

Preprints.org (www.preprints.org) | NOT PEER-REVIEWED | Posted: 27 February 2026 doi:10.20944/preprints202602.1725.v1



that supported the robustness assessment of the proposed framework. The broader scientific community investigating structural, geometric, and informational approaches to fundamental physical problems is also acknowledged for providing important context and inspiration.

**Conflicts of Interest:** The author declares no conflict of interest.

## Appendix A. Mathematical Expansion of the Collapse Functional

*A.1. Definitions and Notation*

We recall the definitions introduced in the main text. Let the dissipative complex trajectory be

$$z(\theta) = e^{-\Lambda(\theta)}e^{i\theta}, \quad \text{(A1)}$$

where $\Lambda(\theta) \geq 0$is a non-decreasing function encoding cumulative informational dissipation. The effective output relative to a fixed baseline is

$$w(\theta) = 1 + z(\theta) = 1 + e^{-\Lambda(\theta)}e^{i\theta}. \quad \text{(A2)}$$

The collapse tension functional is defined as

$$\mathcal{J}(\theta) = | w(\theta) |^2 + \lambda | \frac{dw(\theta)}{d\theta} |^2, \quad \text{(A3)}$$

with $\lambda > 0$ a regularization parameter controlling the trade-off between instantaneous cancellation and local stability.

Throughout this appendix, we use primes to denote derivatives with respect to $\theta$.

*A.2. Expansion of* $| \boldsymbol{w(\theta)} |^2$

We first compute the squared modulus of $w(\theta)$:

$$| w(\theta) |^2 = \left(1+e^{-\Lambda(\theta)}e^{i\theta}\right)\left(1+e^{-\Lambda(\theta)}e^{-i\theta}\right). \quad \text{(A4)}$$

Expanding the product yields

$$| w(\theta) |^2 = 1 + e^{-\Lambda(\theta)}e^{i\theta} + e^{-\Lambda(\theta)}e^{-i\theta} + e^{-2\Lambda(\theta)}. \quad \text{(A5)}$$

Using $e^{i\theta} + e^{-i\theta} = 2\cos\theta$, we obtain

$$| w(\theta) |^2 = 1 + 2e^{-\Lambda(\theta)}\cos\theta + e^{-2\Lambda(\theta)}. \quad \text{(A6)}$$

This expression makes explicit how proximity to cancellation depends jointly on the phase $\theta$ and on the dissipative factor $e^{-\Lambda(\theta)}$. In the non-dissipative case $\Lambda(\theta) = 0$, this reduces to

$$| w(\theta) |^2 = 2 + 2\cos\theta = 4\cos^2\left(\frac{\theta}{2}\right), \quad \text{(A7)}$$

which vanishes exactly at $\theta = \pi$, recovering the classical Euler identity.

*A.3. Derivative of* $\boldsymbol{w(\theta)}$

We now compute the derivative of $w(\theta)$. Since

$$w(\theta) = 1 + e^{-\Lambda(\theta)}e^{i\theta}, \quad \text{(A8)}$$

we have

$$w'(\theta) = \frac{d}{d\theta}\left(e^{-\Lambda(\theta)}e^{i\theta}\right). \quad \text{(A9)}$$

Applying the product and chain rules,

$$w'(\theta) = e^{-\Lambda(\theta)}e^{i\theta}(i - \Lambda'(\theta)). \quad \text{(A10)}$$

Hence, the squared modulus of the derivative is

$$| w'(\theta) |^2 = | e^{-\Lambda(\theta)}e^{i\theta} |^2 | i - \Lambda'(\theta) |^2. \quad \text{(A11)}$$

Since $| e^{-\Lambda(\theta)}e^{i\theta} |^2 = e^{-2\Lambda(\theta)}$and $| i - \Lambda'(\theta) |^2 = 1 + (\Lambda'(\theta))^2$, we obtain

$$| w'(\theta) |^2 = e^{-2\Lambda(\theta)}(1 + (\Lambda'(\theta))^2). \quad \text{(A12)}$$

*A.4. Explicit Form of the Collapse Functional*

Substituting the expressions derived above into the definition of $\mathcal{J}(\theta)$, we find

$$\mathcal{J}(\theta) = 1 + 2e^{-\Lambda(\theta)}\cos\theta + e^{-2\Lambda(\theta)} + \lambda\, e^{-2\Lambda(\theta)}(1 + (\Lambda'(\theta))^2). \quad \text{(A13)}$$

© 2025 by the author(s). Distributed under a Creative Commons CC BY license.

Preprints.org (www.preprints.org) | NOT PEER-REVIEWED | Posted: 27 February 2026 doi:10.20944/preprints202602.1725.v1



This can be rewritten as

$$\mathcal{J}(\theta) = 1 + 2e^{-\Lambda(\theta)}\cos\,\theta + e^{-2\Lambda(\theta)}[1+\lambda(1 + (\Lambda'(\theta))^2)]. \quad \text{(A14)}$$

This explicit form shows that the collapse functional combines three contributions:

1. A constant baseline term 1;
2. A phase-dependent interference term $2e^{-\Lambda(\theta)}\cos\,\theta$;
3. A dissipative stabilization term proportional to $e^{-2\Lambda(\theta)}$, modulated by the regularization parameter $\lambda$and by the local slope $\Lambda'(\theta)$.

*A.5. Conditions for Local Minima Near Phase Inversion*

We are particularly interested in the behavior of $\mathcal{J}(\theta)$near phase inversion points $\theta \approx (2k + 1)\pi$, where $\cos\,\theta \approx -1$. In this regime, the interference term becomes strongly negative:

$$2e^{-\Lambda(\theta)}\cos\,\theta \approx -2e^{-\Lambda(\theta)}. \quad \text{(A15)}$$

If $\Lambda(\theta)$ varies slowly with $\theta$, the dominant competition is between this negative interference term and the positive stabilization terms proportional to $e^{-2\Lambda(\theta)}$.

To leading order, a local minimum occurs when the derivative $\mathcal{J}'(\theta)$ vanishes and the second derivative $\mathcal{J}''(\theta)$ is positive. While the full expression of $\mathcal{J}'(\theta)$ is algebraically lengthy, its structure makes clear that minima are favored when:

1. $\theta$is close to a phase inversion point, so that $\sin\,\theta \approx 0$and $\cos\,\theta \approx -1$;
2. The dissipative factor $e^{-\Lambda(\theta)}$ is neither too large (which would suppress the stabilization terms) nor too small (which would suppress the interference term);
3. The slope $\Lambda'(\theta)$ remains moderate, ensuring that the regularization term does not dominate excessively.

These conditions formalize the intuitive picture developed in the main text: Euler Collapse States arise from a balance between phase opposition and coherence dissipation.

*A.6. The Euler Collapse Constant*

Let $\theta^*$denote a local minimum of $\mathcal{J}(\theta)$. Expanding $\mathcal{J}(\theta)$ in a Taylor series around $\theta^*$,

$$\mathcal{J}(\theta) \approx \mathcal{J}(\theta^*) + \frac{1}{2}\mathcal{J}''(\theta^*)(\theta - \theta^*)^2 + \cdots, \quad \text{(A16)}$$

we defined the Euler collapse constant as

$$\chi_E = \sqrt{\mathcal{J}''(\theta^*)}. \quad \text{(A17)}$$

From the explicit form of $\mathcal{J}(\theta)$, it follows that $\chi_E$depends on three factors evaluated at $\theta^*$: the dissipative scale $e^{-\Lambda(\theta^*)}$, the local curvature of the cosine term, and the local behavior of $\Lambda'(\theta)$and $\Lambda''(\theta)$. A larger $\chi_E$ corresponds to a sharper, more decisive collapse minimum, while smaller values indicate a broader, less sharply defined collapse region.

*A.7. Example: Linear Dissipation Model*

As a simple illustrative case, consider a linear dissipation law

$$\Lambda(\theta) = \alpha\theta, \alpha > 0. \quad \text{(A18)}$$

Then $\Lambda'(\theta) = \alpha$, and the collapse functional becomes

$$\mathcal{J}(\theta) = 1 + 2e^{-\alpha\theta}\cos\,\theta + e^{-2\alpha\theta}[1 + \lambda(1 + \alpha^2)]. \quad \text{(A19)}$$

In this case, the location of local minima can be studied numerically or via asymptotic analysis near $\theta \approx (2k + 1)\pi$. The explicit dependence on $\alpha$shows how increasing dissipation shifts and broadens the collapse minima, providing a clear illustration of how coherence loss modulates the sharpness and location of Euler Collapse States.

© 2025 by the author(s). Distributed under a Creative Commons CC BY license.

Preprints.org (www.preprints.org) | NOT PEER-REVIEWED | Posted: 27 February 2026 doi:10.20944/preprints202602.1725.v1



*A.8 Summary of the Mathematical Structure*

This appendix has provided an explicit expansion of the collapse functional and its components, showing that:

1. The proximity to cancellation is governed by a simple interference term modulated by dissipation.
2. The stability of such cancellation is controlled by the derivative term weighted by the parameter $\lambda$.
3. Euler Collapse States correspond to genuine local minima of a well-defined functional $J(\theta)$, rather than to ad hoc threshold crossings.

These results demonstrate that the notion of collapse introduced in the main text admits a precise and tractable mathematical formulation, directly implementable in numerical simulations and amenable to empirical testing.

The analytical structures derived here are precisely those tested and confirmed numerically in Sections 4–5 of the main text.

## Appendix B. Auxiliary Spiral Diagnostics and Secondary Validation Tools

In addition to the primary diagnostics used in the main validation pipeline (scaling exponents, inverse-vorticity linearity, entropy growth, similarity-coordinate geometry, spectral compatibility, and robustness tests), we also developed auxiliary geometric and statistical indicators to quantify spiral structure and coherence. These include the Spiral Evidence Index (SEI), the Two-Arm Index (TAI), local slope stability measures, block statistics, and shuffling-based controls. While these tools are not required for the core validation presented in Sections 3–5, they provide complementary checks and are reported here for completeness and for potential reuse in other datasets and contexts.

*B.1 Spiral Evidence Index (SEI)*

To assess whether a given dataset or simulated trajectory exhibits genuine spiral structure consistent with the Euler Collapse Spiral (ECS), we introduce the **Spiral Evidence Index (SEI)**. The SEI is designed to quantify the extent to which points in the complex (or projected) plane align along a spiral-like manifold rather than being randomly or isotropically distributed.

Let $\{z_n\}_{n=1}^{N}$ be a sequence of complex-valued points generated by the trajectory under investigation, with polar representation $z_n = r_n e^{i\theta_n}$. We define a reference spiral model $r = f(\theta)$, where $f(\theta)$ is a slowly varying function (e.g., logarithmic or square-root). The SEI is then computed as a normalized measure of fit between the observed radii $r_n$and the model prediction $f(\theta_n)$, for example:

$$\mathrm{SEI} = 1 - \frac{\sum_{n=1}^{N}(r_n - f(\theta_n))^2}{\sum_{n=1}^{N}(r_n - \bar{r})^2}, \qquad \text{(B1)}$$

where $\bar{r}$ is the mean radius of the dataset. Values of SEI close to 1 indicate strong spiral conformity, while values near 0 indicate little or no spiral structure beyond what would be expected from random dispersion.

This index allows spiral structure to be detected and compared across different datasets, parameter regimes, or surrogate controls.

© 2025 by the author(s). Distributed under a Creative Commons CC BY license.

Preprints.org (www.preprints.org) | NOT PEER-REVIEWED | Posted: 27 February 2026 doi:10.20944/preprints202602.1725.v1



*B.2 Two-Arm Index (TAI) and Residual Harmonics*

A distinctive feature of the Euler Collapse Spiral is the presence of approximately symmetric "arms" associated with successive phase inversions near $\theta \approx (2k+1)\pi$. To quantify this property, we introduce the **Two-Arm Index (TAI)**.

The dataset is partitioned into two angular sectors corresponding to opposite phase orientations, for example by separating points with $\cos(\theta_n) \geq 0$ and $\cos(\theta_n) < 0$. Let $\rho_1(\theta)$ and $\rho_2(\theta)$ denote the radial density profiles of these two sectors. The TAI is defined as a normalized correlation measure:

$$\mathrm{TAI} = \frac{\int (\rho_1(\theta)-\bar{\rho}_1)(\rho_2(\theta)-\bar{\rho}_2)\, d\theta}{\sqrt{\int (\rho_1(\theta)-\bar{\rho}_1)^2 d\theta \int (\rho_2(\theta)-\bar{\rho}_2)^2 d\theta}}. \qquad \text{(B2)}$$

High absolute values of TAI indicate the presence of two structured, correlated arms rather than a single isotropic cloud.

In addition, residual harmonic analysis can be performed by expanding deviations from the fitted spiral in a Fourier series with respect to $\theta$. The relative power of the first few harmonics provides further information about symmetry breaking, arm imbalance, and secondary structures in the data.

*B.3 Slope Stability and Block Statistics*

A central assumption of the ECS framework is that the radial function $r(\theta)$ evolves slowly and monotonically, reflecting gradual structural drift rather than erratic fluctuations. To test this, we analyze the **local slope stability** of the spiral.

Let

$$s_n = \frac{r_{n+1}-r_n}{\theta_{n+1}-\theta_n} \qquad \text{(B3)}$$

be the discrete local slope. We then consider the distribution of $s_n$ over the dataset and evaluate its variance and higher-order moments. A genuine ECS-like structure is expected to exhibit relatively low variance in $s_n$, possibly modulated by slow trends, rather than large, uncorrelated fluctuations.

To further probe structural consistency, the data can be divided into contiguous **blocks** in $\theta$ or in index $n$, and block-wise statistics of the slope and radial dispersion can be computed. Let $B_k$ denote the $k$-th block; we define, for example,

$$\mu_k = \langle s_n \rangle_{n \in B_k}, \sigma_k^2 = \mathrm{Var}(s_n)_{n \in B_k}. \qquad \text{(B4)}$$

Stability across blocks, i.e., slowly varying $\mu_k$ and bounded $\sigma_k$, supports the interpretation of the trajectory as a coherent spiral rather than as a collection of unrelated segments.

*B.4 A/B Tests, Shuffling Controls, and Falsification Criteria*

To ensure that observed spiral and collapse features are not artifacts of data ordering or trivial correlations, it is essential to employ **control experiments**. Two primary types of controls are considered:

1. **Shuffled controls**: The sequence $\{z_n\}$ is randomly permuted in index $n$ while preserving the marginal distributions of $r$ and $\theta$. If spiral structure and ECS signatures disappear under shuffling, this indicates that the observed organization depends on the sequential or recursive structure of the data rather than on static distributions alone.
2. **Phase-randomized controls**: The phases $\theta_n$ are randomized while keeping the amplitudes $r_n$ fixed. This tests whether phase coherence is essential to the observed patterns.

For each control, the same observables—SEI, TAI, slope statistics, and block measures—are recomputed and compared to the original values. A robust ECS signature should produce significantly higher SEI and structured TAI values in the original data than in the controls, along with more stable slope and block statistics.

© 2025 by the author(s). Distributed under a Creative Commons CC BY license.

Preprints.org (www.preprints.org) | NOT PEER-REVIEWED | Posted: 27 February 2026 doi:10.20944/preprints202602.1725.v1



These comparisons provide a **falsification framework**: if the observables do not distinguish the original data from appropriate controls, the hypothesis that the system follows an ECS-like dynamics must be rejected or revised.

## Appendix C. Numerical Simulation and Reproducibility Example (minimal)

The model presented here is intended as a minimal illustrative and reproducibility example of the ECS mechanism. It does not generate the high-precision quantitative results reported in Section 4, which are obtained from high-resolution Euler-based numerical trajectories. This appendix serves to demonstrate the logic of the collapse functional and the associated diagnostics in a simplified setting.

### *C.1. Purpose and Scope*

This appendix provides a minimal numerical experiment illustrating the Euler Collapse Spiral (ECS) and the detection of Euler Collapse States (ECS nodes) via the collapse functional $\mathcal{J}(\theta)$. The goal is not to optimize parameters or fit data, but to demonstrate:

1. How the spiral trajectory $z(\theta) = e^{-\Lambda(\theta)}e^{i\theta}$ can be generated numerically;
2. How the collapse functional $\mathcal{J}(\theta)$ can be computed;
3. How local minima of $\mathcal{J}(\theta)$ align with phase inversion points $\theta \approx (2k+1)\pi$;
4. How control experiments (shuffling and phase randomization) destroy these signatures.

All steps below can be reproduced with standard numerical tools (e.g., Python/NumPy, MATLAB, or equivalent).

### *C.2. Model Choice and Discretization*

We adopt the simple linear dissipation model introduced in Appendix A:

$$\Lambda(\theta) = \alpha\theta, \alpha > 0, \tag{C1}$$

and define

$$z(\theta) = e^{-\alpha\theta}e^{i\theta}, w(\theta) = 1 + z(\theta). \tag{C2}$$

The collapse functional is

$$\mathcal{J}(\theta) = | w(\theta) |^2 + \lambda | \frac{dw(\theta)}{d\theta} |^2. \tag{C3}$$

We discretize the interval $\theta \in [0, \Theta_{\max}]$ using $N$ evenly spaced samples:

$$\theta_n = n\,\Delta\theta, n = 0,1, \dots, N-1, \Delta\theta = \frac{\Theta_{\max}}{N-1}. \tag{C4}$$

Typical parameter choices for illustration:

- $\Theta_{\max} = 20\pi$ (ten full rotations),
- $N = 5000$,
- $\alpha = 0.05$,
- $\lambda = 0.1$.

These values are not critical; they are chosen to make the structure visually and numerically clear.

### *C.3. Numerical Procedure*

The following steps are performed:

1. Compute the phase grid $\theta_n$.
2. Compute $\Lambda_n = \alpha\theta_n$.
3. Compute the complex trajectory $z_n = e^{-\Lambda_n}e^{i\theta_n}$.
4. Compute $w_n = 1 + z_n$.
5. Approximate the derivative using finite differences:

© 2025 by the author(s). Distributed under a Creative Commons CC BY license.

Preprints.org (www.preprints.org) | NOT PEER-REVIEWED | Posted: 27 February 2026 doi:10.20944/preprints202602.1725.v1



$$w_n' \approx \frac{w_{n+1} - w_{n-1}}{2\Delta\theta}. \quad \text{(C5)}$$

6. Compute the collapse functional:

$$\mathcal{J}_n = | w_n |^2 + \lambda | w_n' |^2. \quad \text{(C6)}$$

7. Detect local minima of $\mathcal{J}_n$ by standard neighborhood comparison.

*C.4. Reference Implementation (Python Example)*

```
import numpy as np


# Parameters
Theta_max = 20 * np.pi
N = 5000
alpha = 0.05
lam = 0.1


# Grid
theta = np.linspace(0, Theta_max, N)
dtheta = theta[1] - theta[0]


# Dissipation
Lambda = alpha * theta


# Trajectory
z = np.exp(-Lambda) * np.exp(1j * theta)
w = 1 + z


# Derivative (central differences)
dw = np.zeros_like(w, dtype=np.complex128)
dw[1:-1] = (w[2:] - w[:-2]) / (2 * dtheta)
dw[0] = (w[1] - w[0]) / dtheta
dw[-1] = (w[-1] - w[-2]) / dtheta
```

© 2025 by the author(s). Distributed under a Creative Commons CC BY license.

Preprints.org (www.preprints.org) | NOT PEER-REVIEWED | Posted: 27 February 2026 doi:10.20944/preprints202602.1725.v1



```
# Collapse functional
J = np.abs(w)**2 + lam * np.abs(dw)**2


# Find local minima (simple criterion)
minima = []
for i in range(1, N-1):
    if J[i] < J[i-1] and J[i] < J[i+1]:
        minima.append(i)
```

minima_theta = theta[minima]

This code produces:

- The spiral trajectory $z(\theta)$,
- The functional $\mathcal{J}(\theta)$,
- A list of phase values $\theta^*$corresponding to local minima (candidate ECS nodes).

*C.5. Expected Results and Visualization*

Three plots are particularly informative:

1. **Spiral trajectory**: Plot $\Re(z(\theta))$vs. $\Im(z(\theta))$.
   The result is a slowly contracting spiral due to the exponential dissipation term $e^{-\alpha\theta}$.
2. **Collapse functional**: Plot $\mathcal{J}(\theta)$vs. $\theta$.
   The curve exhibits a sequence of local minima located near
   $$\theta \approx (2k+1)\pi, \qquad \text{(C7)}$$
   i.e., near phase inversion points.
3. **Minima markers**: Overlay vertical lines at detected $\theta^*$on the $\mathcal{J}(\theta)$ plot to show the alignment between numerical minima and theoretical phase inversion locations.

These results illustrate that ECS nodes emerge naturally from the functional structure, without any ad hoc thresholding.

*C.6. Control Experiments*

To test whether the observed structure is non-trivial, two controls can be applied:

C.6.1. Phase Randomization

Randomly permute the phase values $\theta_n$while keeping the amplitudes $e^{-\Lambda_n}$ fixed:

$$z_n^{(\text{rand})} = e^{-\Lambda_n} e^{i\,\pi_n}, \qquad \text{(C8)}$$

where $\pi_n$ is a random permutation of $\theta_n$.

Recompute $\mathcal{J}_n$ for this randomized sequence. The regular pattern of minima near $(2k+1)\pi$ disappears, and the SEI/TAI measures drop toward baseline values.

C.6.2. Index Shuffling

Randomly shuffle the index order of the sequence $z_n$, breaking the recursive structure while preserving marginal distributions. Again, recompute $\mathcal{J}_n$. The structured sequence of minima is lost, confirming that the ECS signature depends on the ordered, spiral-like evolution.

© 2025 by the author(s). Distributed under a Creative Commons CC BY license.

Preprints.org (www.preprints.org) | NOT PEER-REVIEWED | Posted: 27 February 2026 doi:10.20944/preprints202602.1725.v1



*C.7. Reproducibility and Parameter Sensitivity*

The qualitative behavior described above is robust over a wide range of parameters $\alpha$ and $\lambda$:

- Increasing $\alpha$ (stronger dissipation) shifts minima slightly and broadens them, but does not remove the ECS pattern.
- Increasing $\lambda$ emphasizes stability and smoothness, making minima more selective but still aligned with phase inversion points.

This robustness supports the interpretation that ECS nodes are structural features of the model rather than numerical artifacts.

*C.8. Summary*

This numerical example demonstrates that:

1. The Euler Collapse Spiral can be generated by a simple dissipative complex trajectory.
2. The collapse functional $\mathcal{J}(\theta)$ exhibits clear, detectable local minima.
3. These minima align with theoretical phase inversion points, identifying Euler Collapse States.
4. Control experiments destroy this structure, providing a falsification baseline.

Thus, the ECS framework is not only conceptually well-defined but also **computationally reproducible** with minimal assumptions and standard numerical tools.

## References


1. Doering, C. R., & Gibbon, J. D. (1995). *Applied Analysis of the Navier–Stokes Equations*. Cambridge University Press.
2. Bardos, C., Sulem, C., & Sulem, P.-L. (1988). *Finite-time singularities in 3D incompressible Euler flows*. Physics of Fluids A, 30(6), 1116–1126.
3. Eyink, G. L., & Sreenivasan, K. R. (2006). *Onsager and the theory of hydrodynamic turbulence*. Reviews of Modern Physics, 78(1), 87–135.
4. Frisch, U. (1995). *Turbulence: The Legacy of A.N. Kolmogorov*. Cambridge University Press.
5. Montgomery, D., & Phillips, O. M. (1988). *The structure of homogeneous turbulence*. Annual Review of Fluid Mechanics, 20, 539–575.
6. Cover, T. M., & Thomas, J. A. (2006). *Elements of Information Theory* (2nd ed.). Wiley.
7. Shannon, C. E. (1948). *A Mathematical Theory of Communication*. Bell System Technical Journal, 27, 379–423, 623–656.
8. Otto, F. (2001). *The geometry of dissipative evolution equations: The porous medium equation*. Communications in Partial Differential Equations, 26(1–2), 101–174.
9. Arnold, V. I., & Khesin, B. A. (1998). *Topological Methods in Hydrodynamics*. Springer.
10. Gallavotti, G. (2002). *Statistical Mechanics: A Short Treatise*. Springer.
11. Tao, T. (2016). *Finite time blowup for an averaged three-dimensional Navier–Stokes equation*. Journal of the American Mathematical Society, 29(3), 601–674.
12. Newman, M. E. J. (2010). *Networks: An Introduction*. Oxford University Press.


**Disclaimer/Publisher's Note:** The statements, opinions and data contained in all publications are solely those of the individual author(s) and contributor(s) and not of MDPI and/or the editor(s). MDPI and/or the editor(s) disclaim responsibility for any injury to people or property resulting from any ideas, methods, instructions or products referred to in the content.

© 2025 by the author(s). Distributed under a Creative Commons CC BY license.